# Electronic Supplementary Information

## Halobenzyl Alcohols as Structurally Simple Organogelators

Annamalai Prathap, Arthi Ravi, Javed R. Pathan and Kana M. Sureshan*

School of Chemistry, Indian Institute of Science Education and Research Thiruvananthapuram, Maruthamala (P.O), Vithura, Kerala, India - 695551. E-mail: kms@iisertvm.ac.in

### Materials and Methods

All the halogen substituted benzyl alcohols were purchased from TCI and Sigma Aldrich and were used as such for performing gel studies. Commercial solvents were purchased from Aldrich chemicals and used as such. Diesel (cetane number 45-55) and Petrol (octane number 85-88) were purchased from gas outlets (Bharat petroleum) and used as such. Rheology analyses of the gels were performed using a Modular Compact Rheometer (MCR 302) by Anton Paar using parallel plate configuration (PP25). All gel samples used for rheology analyses were of same concentration (1M in hexadecane).

Single crystal X-ray diffraction analyses of compounds **3**, **6**, **7**, **9**, **10** and **11** were performed using a Bruker-KAPPA APEX II CCD diffractometer in omega and phi scan mode, MoKα = 0.71073 Å. Data reduction was carried out with the SAINT/XREP (Bruker 2016) software package. The absorption corrections and the correction of other systematic errors were carried out with SADABS (Bruker 2016). Structures were solved using SHELXT 2014/5. Least squares refinement was carried out with SHELXL-2014.[1,2] The H-atom positions were fixed using riding models. In the case of compounds **3**, **9** and **11**, the hydrogen atom positions on the oxygen atoms were positioned geometrically, fitted into a 50:50 disorder model, and restraints applied during refinement. In case of compound **6**, several atom positions were found to be disordered. These were modelled, the ratio of their site occupancy factors determined, and suitable geometric restraints were applied. But, in this heavy-atom structure as it was not possible to see clear electron-density peaks in difference maps which would correspond with acceptable locations for the various disordered hydroxy H atoms, the refinement was completed with no allowance for these hydroxy H atoms in the models. Face-indexing of single crystals of compounds **3**, **6**, **7**, **9**, **10** and **11** was carried out using Bruker AXS Face-indexing User Interface after data collection from a Bruker KAPPA APEX-II diffractometer in omega and phi scan mode, MoKα = 0.71073 Å. Powder patterns were simulated from SCXRD structures using Mercury 4.1.2. The Bravais-Friedel-Donnay-Harker (BFDH) crystal morphology with (hkl) indices was calculated using Mercury 4.1.2. The morphology was calculated taking into account the attachment surface energy using the program, *Oscail.*[3] The faces with the highest attachement energy *i.e.* lowest morphological dominance, grow fast.[4]

PXRD analyses were performed using Bruker PANalytical. The PXRD experiments were conducted using slow and continuous scan rate mode using Cu as the anode material ($K\alpha_1$ = 1.540598Å). Fresh wet gels made by the gelators **1**-**11** in hexadecane solvents (0.2M) were taken in a glass slide and the PXRD experiment was conducted. Xerogels were prepared by lyophilisation of octane gels in ScanVac Coolsafe 110-4 instrument and used in PXRD analysis. IR spectra were recorded on an IR Prestige-21 instrument by placing the gel in the ATR holder. A small piece of gel was placed on the ATR crystal after collecting the background with gelling solvent and then the spectra were recorded. IR spectra of

chloroform solutions of the gelators were recorded in a NaCl cell, and gel samples were recorded by mixing with KBr and making a pellet. SEM images were recorded by using a JEOL JSM-5600LV scanning electron microscope. A small piece of xerogel was placed on carbon tape pasted to a steel grid, sputter coated with chromium, and then directly imaged under the scanning electron microscope.

### Gelation and Critical Gelation Concentration (CGC) Analysis

20 mg of gelator taken in a vial was dissolved in 1 mL of solvent by heating and the hot homogeneous solution was instantaneously cooled to 10 °C by immersing the vial in ice water. If the solution turned into gel (CGC = 2 wt%), a measured volume of solvent was added and checked again for its gelation until there is no further gel formation. The maximum amount of solvent that could be congealed by the 20 mg of gelator was noted and the CGC was calculated using the formula CGC = [weight of gelator (gram)/volume (mL) ]x 100.

### Gel melting temperature ($T_{gel}$) analysis

8 wt % of hexadecane gel was prepared in a 5 mL test tube and the gel was heated slowly (2 °C/min) in an oil bath. The $T_{gel}$ was determined by adopting the inverted vial test as reported.[5]

### Rheology analysis

Hexadecane gels of 1M and 200 mM concentrations were prepared separately for compounds **1**-**11** by heating-cooling method. A small portion of the freshly prepared gel was placed on the rheometer using a spatula and the rheology was done in amplitude sweep followed by frequency sweep using parallel plate system (PP25). Storage (G') and loss moduli (G'') were obtained in frequency sweep mode using 0.01% strain for all the samples.

### Crystallization

5 mL of 1M Hexadecane gels formed by the compounds **3**, **6**, **7**, **9**, **10** and **11** were left in open condition for about a month. Upon slow evaporation of the solvent, the thick fibers of the gels turned into crystalline fibers after a month. Good quality crystals were picked up for the single crystal X – ray diffraction analysis.

### Xerogel preparation

1 mL of 6 wt% of gel was prepared using either octane or hexadecane by heating followed by rapidly cooling by immersing in ice water. The gel formed was frozen by placing the gel vial in liquid nitrogen for about 4 hours. The frozen sample was freeze-dried using lyophilizer for about 5-6 hours.

**Table S1** CGC data of gelators **1**-**11** in wt%. The value in parenthesis is the concentration in mM.

| | 1 | 2 | 3 | 4 | 5 | 6 | 7 | 8 | 9 | 10 | 11 |
|---|---|---|---|---|---|---|---|---|---|---|---|

| | | | | | | | | | | | |
|---|---|---|---|---|---|---|---|---|---|---|---|
| Heptane | 0.9 (63) | 0.9(48) | 0.8(32) | 0.9(63) | 0.8(44) | 0.8(35) | 0.7(43) | 1.4(79) | 0.9(51) | 1(56) | 1(38) |
| n-Octane | 1.3(88) | 1.2(59) | 1(43) | 2(141) | 1.3(67) | 0.8(35) | 0.8(47) | 2(113) | 1.5(80) | 1.3(71) | 1.3(47) |
| Undecane | 1.3(88) | 1.2(59) | 1.2(47) | 1.2(78) | 1.3(67) | 1.2(47) | 0.9(51) | 2(113) | 1.3(71) | 1.5(80) | 1.3(47) |
| Dodecane | 2(141) | 2.5(134) | 2.5(107) | 2(141) | 1.7(89) | 1.5(61) | 0.9(51) | 2(113) | 1.5(80) | 1.5(80) | 1.5(54) |
| Hexadecane | 2.5(176) | 1.2(59) | 0.9(38) | 0.9(63) | 1.3(67) | 1.1(47) | 0.7(40) | 2(113) | 1.3(71) | 1.3(71) | 1(38) |
| Cyclo hexane | 5(352) | 2.5(134) | 2(85) | 2(141) | 1.7(89) | 1.7(71) | 1(56) | 5(282) | 4.4(245) | 4.4(245) | 2(75) |
| Diesel | 5(352) | 5 (267) | 2.5(107) | 2.5(176) | 3.4(178) | 2.5(107) | 2(113) | 5(282) | 5(282) | 2.5(141) | 3.4(126) |
| Petrol | 10(704) | 3.4(178) | 3.4(42) | 10(704) | 5(267) | 10(427) | 3.4(188) | 10(565) | 10(565) | 5(282) | 10(377) |
| Toluene* | - | - | - | - | - | - | - | - | - | - | - |
| Styrene* | - | - | - | - | - | - | - | - | - | - | - |
| THF* | - | - | - | - | - | - | - | - | - | - | - |

* In these solvents no gelation was observed.

**Table S2** $T_{gel}$ data in (°C)

| Gelator | **1** | **2** | **3** | **4** | **5** | **6** | **7** | **8** | **9** | **10** | **11** |
|---|---|---|---|---|---|---|---|---|---|---|---|
| Hexadecane | 71.6 | 72.4 | 80.1 | 63.1 | 74.2 | 69.5 | 79.8 | 54 | 68.6 | 78.6 | 66 |

## Rheology analyses

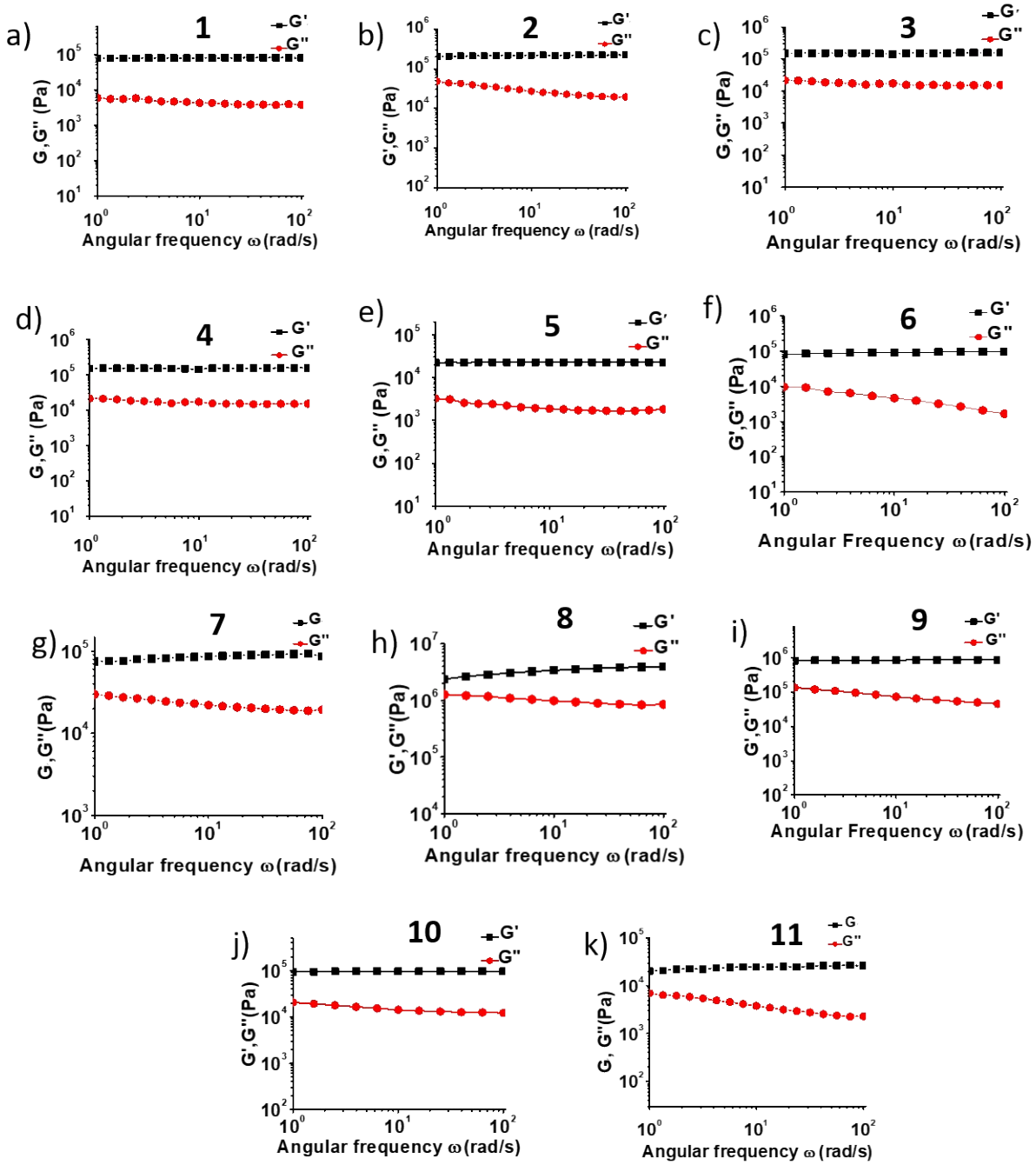


**Fig. S1** Rheograms (frequency sweep mode) a)-k) the storage and loss moduli of 1M hexadecane gels formed by compounds **1**-**11** respectively.

**PXRD analysis**

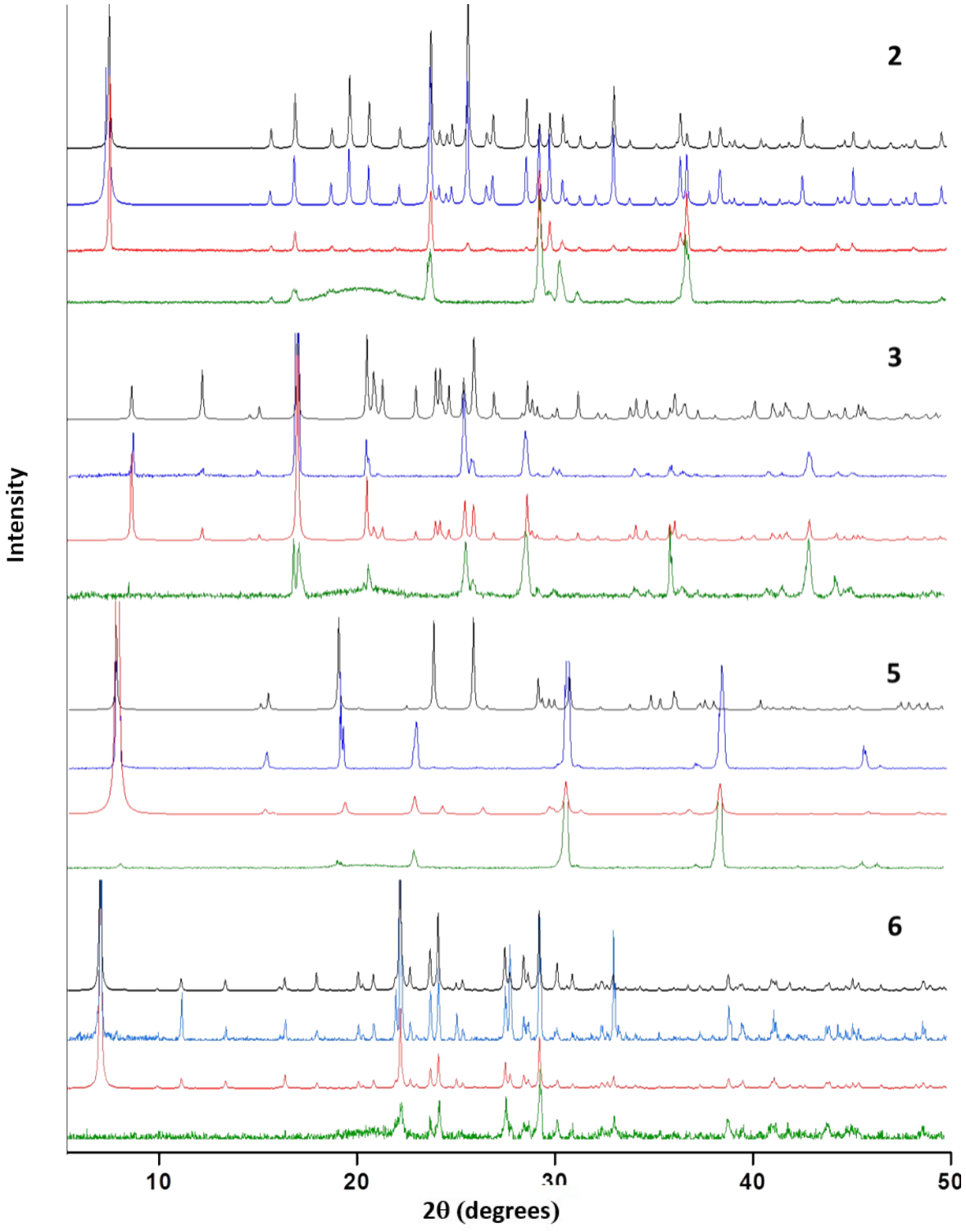


**Fig. S2** Comparison of the PXRD patterns of xerogel (blue) and wet gel (green) with the simulated PXRD patterns generated from the SCXRD data. Patterns corresponding to the bulk crystals are in black and the patterns simulated from the plane formed the parallel alignment of H-bonded chains are in red.

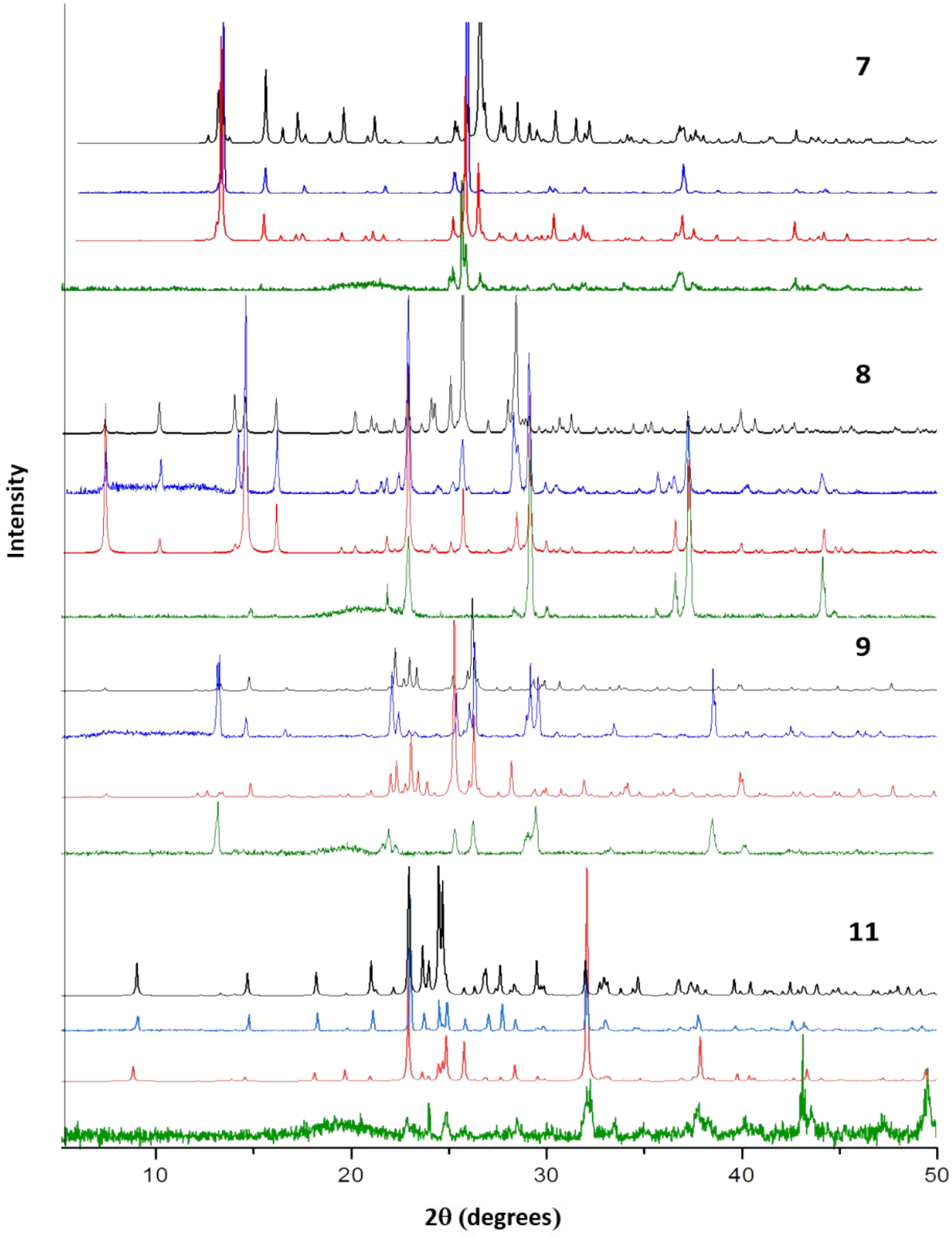


**Fig**. **S3** Comparison of the PXRD patterns of xerogel (blue) and wet gel (green) with the simulated PXRD patterns generated from the SCXRD data. Patterns corresponding to the bulk crystals are in black and the patterns simulated from the plane formed the parallel alignment of H-bonded chains are in red.

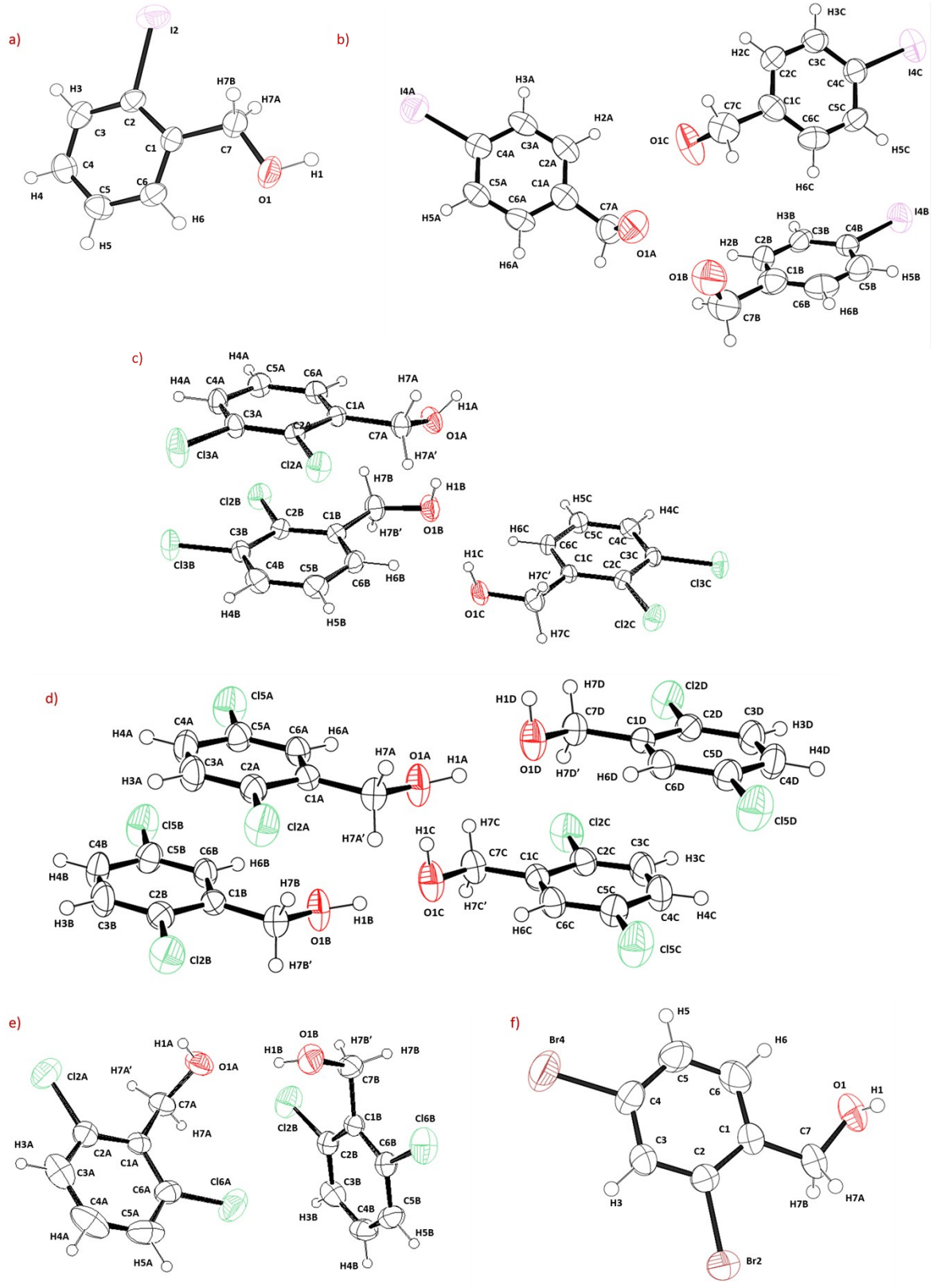


**Fig. S4**. ORTEP diagrams of a) compound **3**, b) compound **6**, c) compound **7**, d) compound **9**, e) compound **10** and f) compound **11**. The thermal ellipsoids are set at 50 % probability. The disordered atoms (in case of compounds **3**, **6 9** and **11**) are omitted for clarity.

**Table S3** Crystal data for Compounds **3**, **6**, **7**, **9**, **10** and **11**.

| | Compound **3** | Compound **6** | Compound **7** | Compound **9** | Compound **10** | Compound **11** |
|---|---|---|---|---|---|---|
| CCDC number | 1881163 | 1881165 | 1881164 | 1881166 | 1881167 | 1881188 |
| Empirical formula | C7 H7 I O | C7 H7 I O | C7H6C12O | C7 H6 Cl2 O | C7 H6 Cl2 O | C7 H6 Br2 O |
| Formula weight | 234.03 | 234.03 | 177.02 | 177.02 | 177.02 | 265.94 |
| Temperature | 296(2) K | 296(2) K | 296(2) K | 296(2) K | 296(2) K | 296(2) K |
| Wavelength | 0.71073 Å | 0.71073 A | 0.71073 A° | 0.71073 Å | 0.71073 Å | 0.71073 Å |
| Crystal system | Monoclinic | Orthorhombic | Triclinic | Triclinic | Triclinic | Monoclinic |
| Space group | P 21/n | P2(1)2(1)2(1) | P -1 | P -1 | P -1 | P 21/c |
| Unit cell dimensions | a = 12.803(9) Å<br>b = 4.630(3) Å<br>c = 13.233(9) Å<br>α = 90°<br>β = 109.94(2)°.<br>γ = 90°. | a = 6.0322(3) A<br>b = 16.5564(10) A<br>c = 22.5967(9) A<br>α = 90 °<br>β = 90°<br>γ = 90°. | a = 7.073(17) Å<br>b = 7.513(19)A°<br>C = 21.13(5) A°<br>α = 92.270(6)°<br>β = 94.494(7)°<br>γ = 94.926(7)° | a = 7.182(4) Å<br>b = 14.930(9) Å<br>c = 15.398(9) Å<br>α = 107.74(18)°.<br>β = 97.26(18)°.<br>γ = 100.10(19)°. | a = 8.2382(14) Å<br>b = 8.6956(14) Å<br>c = 11.674(2) Å<br>α = 83.844(6)°.<br>β = 70.803(5)°.<br>γ = 79.456(5)°. | a = 4.2512(9) Å<br>b = 14.458(3) Å<br>c = 13.500(3) Å<br>α = 90°.<br>β = 97.411(8)°.<br>γ = 90°. |
| Volume | 737.4(9) $Å^3$ | 2256.8(2) $Å^3$ | 1114.5(5) $Å^3$ | 1519.4(15) $Å^3$ | 775.4(2) $Å^3$ | 822.8(3) $Å^3$ |
| Z | 4 | 12 | 6 | 8 | 4 | 4 |
| Density (calculated) | 2.108 $g/cm^3$ | 2.066 $g/cm^3$ | 1.583 $g/cm^3$ | 1.548 $g/cm^3$ | 1.516 $g/cm^3$ | 2.147 $g/cm^3$ |
| Absorption coefficient | 4.257 $mm^{-1}$ | 4.173 $mm^{-1}$ | 0.793 $mm^{-1}$ | 0.775 mm-1 | 0.760 mm-1 | 9.779 mm-1 |
| F(000) | 440 | 1320 | 540 | 720 | 360 | 504 |
| Crystal size ($mm^3$) | 0.200 x 0.100 x 0.050 mm3 | 0.20 x 0.15 x 0.12 mm | 0.240x0.150x0.08 | 0.250 x 0.200 x 0.200 mm3 | 0.250 x 0.150 x 0.150 mm3 | 0.200 x 0.120 x 0.120 mm3 |
| Theta range for data collection | 2.727 to 25.53 | 2.46 to 25.48° | 0.967 to 25.000° | 1.415 to 25.998°. | 1.850 to 25.995°. | 2.818 to 24.995°. |
| Index ranges | -16<=h<=16, -6<=k<=6, -16<=l<=17 | -7<=h<=6, -19<=k<=16, -26<=l<=19 | -8<=h<=8, -8<=k<=8, -25<=l<=25 | -8<=h<=8, -18<=k<=18, -18<=l<=18 | -9<=h<=10, -10<=k<=10, 0<=l<=14 | -5<=h<=5, -17<=k<=17, -14<=l<=16 |
| Reflections collected | 12224 | 10244 | 20488 | 24084 | 3048 | 9356 |
| Independent reflections | 1719 | 3762 | 3925 | 5957 | 3048 | 1435 |
| Completeness to theta = 25.000° | 99.9 % | 99.8 % | 100.0 % | 99.9 % | 100.0 % | 99.9 % |
| Absorption correction | Semi-empirical from equivalents | Semi-empirical from equivalents | Semi-empirical from equivalents | Semi-empirical from equivalents | Semi-empirical from equivalents | Semi-empirical from equivalents |
| Max. and min. transmission | 0.815 and 0.483 | 0.6344 and 0.4891 | 0.939 and 0.833 | 0.860 and 0.830 | 0.895 and 0.833 | 0.387 and 0.245 |
| Refinement method | Full-matrix least-squares on F2 | Full-matrix least-squares on F2 | Full-matrix least-squares on F2 | Full-matrix least-squares on F2 | Full-matrix least-squares on F2 | Full-matrix least-squares on F2 |
| Data / restraints / parameters | 1719 / 3/ 90 | 3762 / 147 / 260 | 3925 / 0 / 274 | 5957 / 9 / 391 | 3048 / 0 / 185 | 1435 / 8/ 107 |
| Goodness-of-fit on F2 | 1.028 | 1.046 | 1.038 | 1.056 | 1.024 | 1.051 |
| Final R indices [I>2sigma(I)] | R1 = 0.0296, wR2 = 0.0612 | R1 = 0.0284, wR2 = 0.0663 | R1 = 0.0513, wR2 = 0.1020 | R1 = 0.04804, wR2 = 0.1215 | R1 = 0.0585, wR2 = 0.1404 | R1 = 0.0369, wR2 = 0.0711 |
| R indices (all data) | R1 = 0.0480, wR2 = 0.0674 | R1 = 0.0351, wR2 = 0.0701 | R1 = 0.0942, wR2 = 0.1206 | R1 = 0.07777, wR2 = 0.1431 | R1 = 0.0809, wR2 = 0.1599 | R1 = 0.0703, wR2 = 0.0817 |
| Extinction coefficient | n/a | n/a | n/a | n/a | 0.059(5) | n/a |
| Largest diff. peak and hole(e.$Å^{-3}$) | 0.621 and -0.602 | 0.656 and -0.512 | 0.252 and -0.290 | 0.353 and -0.245 | 0.657 and -0.496 | 0.616 and -0.361 |

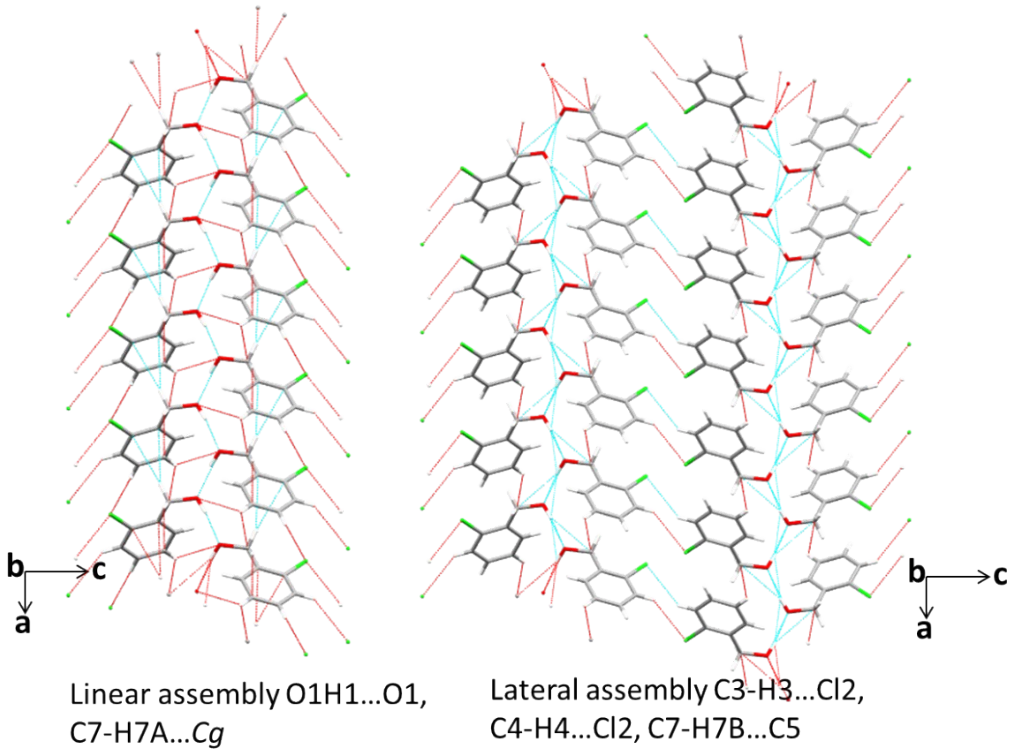


**Fig. S5** Packing diagram showing the linear and lateral assembly in the crystal of compound **1**.

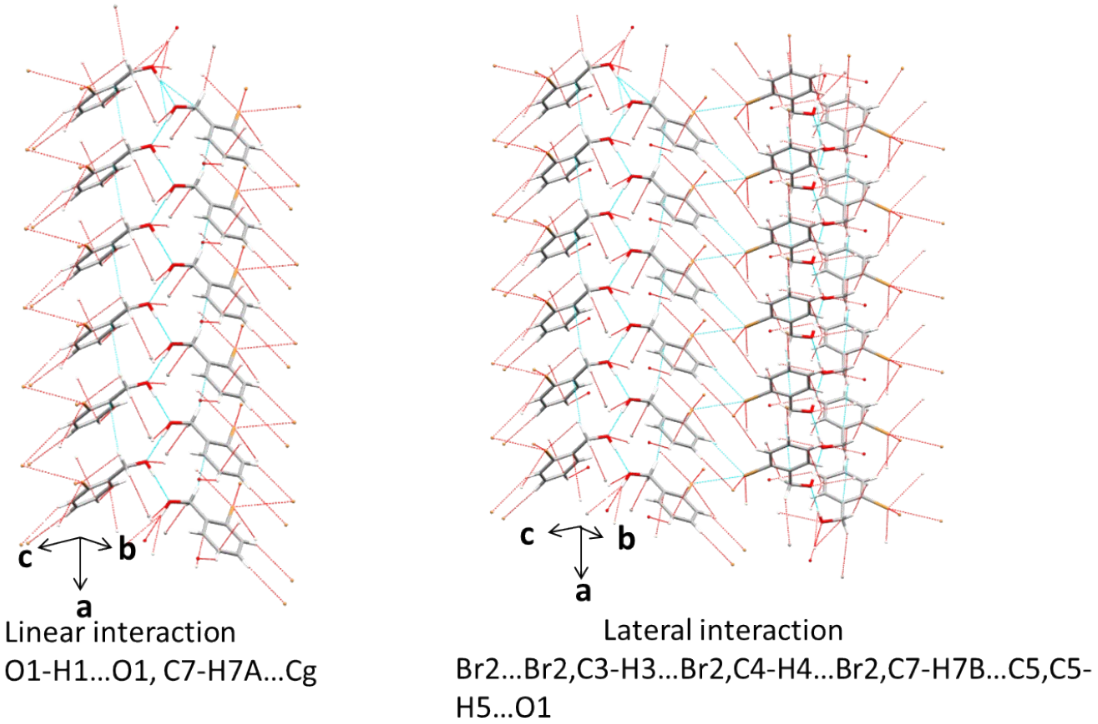


**Fig. S6** Packing diagram showing the linear and lateral assembly in the crystal of compound **2**.

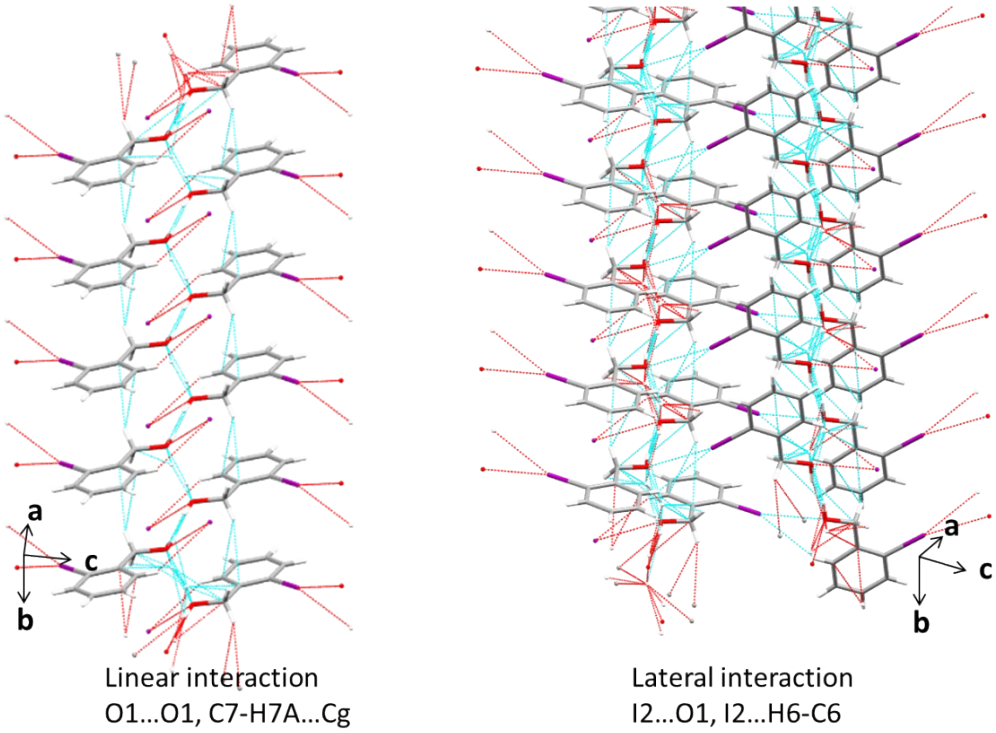


**Fig. S7** Packing diagram showing the linear and lateral assembly in the crystal of compound **3**.

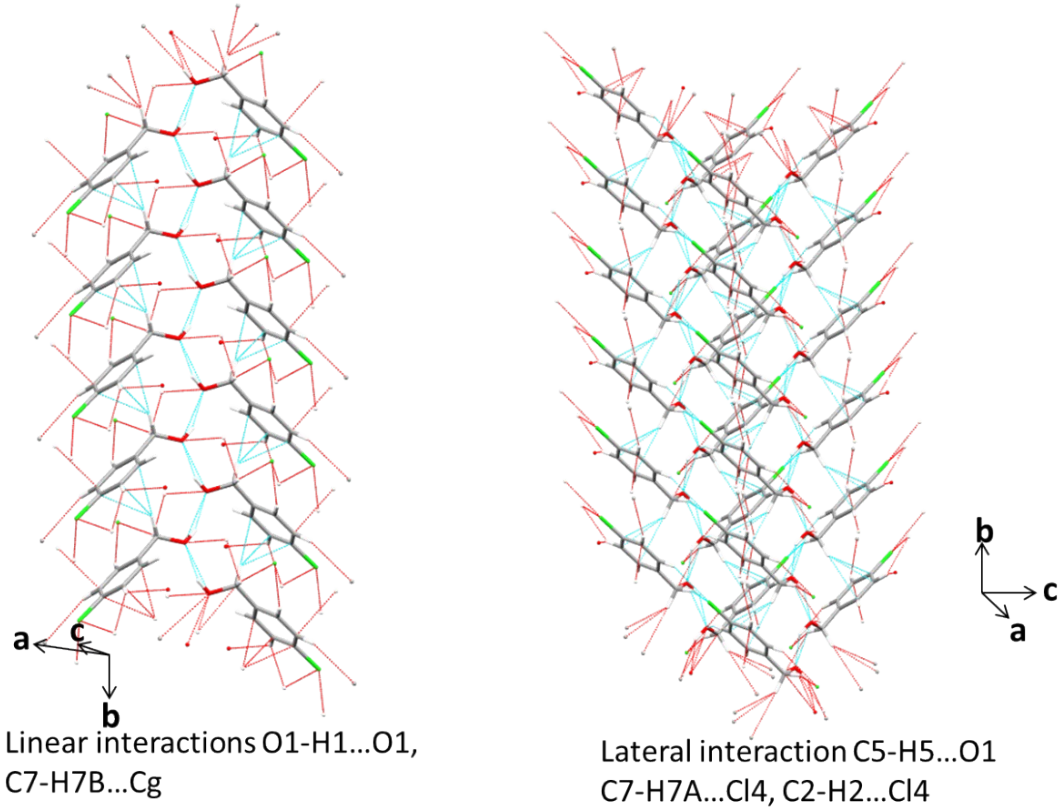


**Fig. S8** Packing diagram showing the linear and lateral assembly in the crystal of compound **4**.

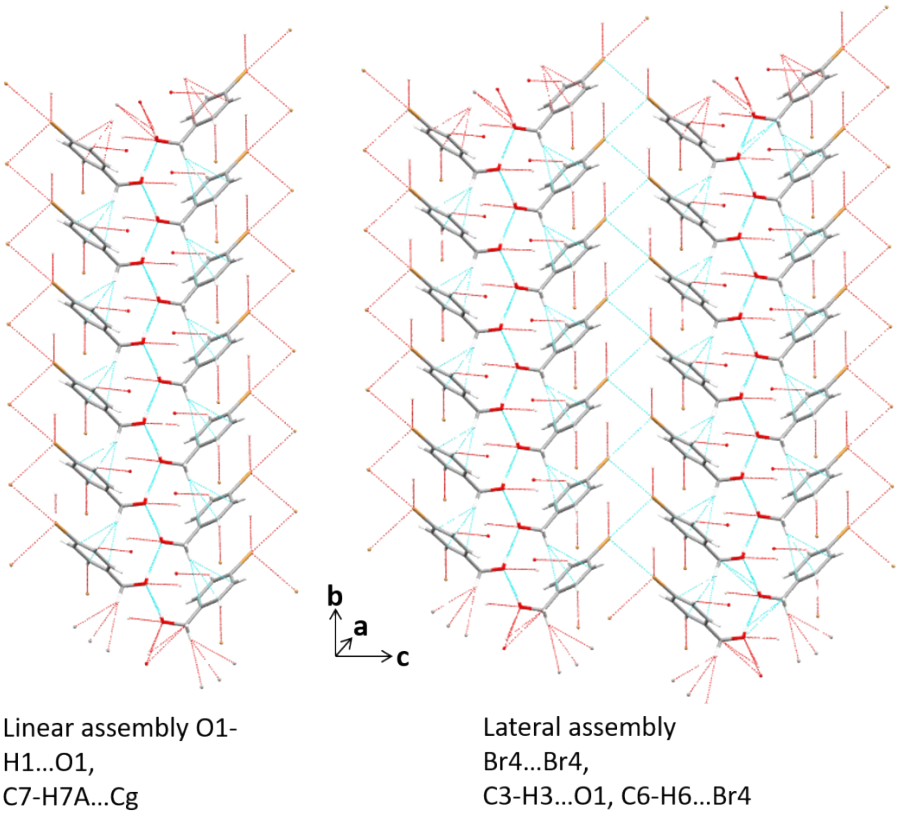


**Fig. S9** Packing diagram showing the linear and lateral assembly in the crystal of compound **5**.

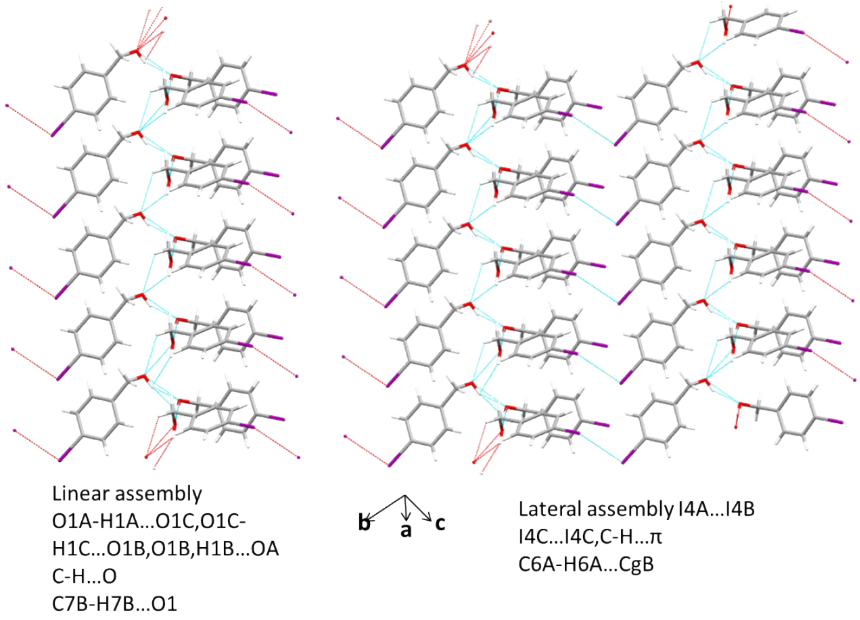


**Fig. S10** Packing diagram showing the linear and lateral assembly in the crystal of compound **6**. The disordered atom are omitted for clarity.

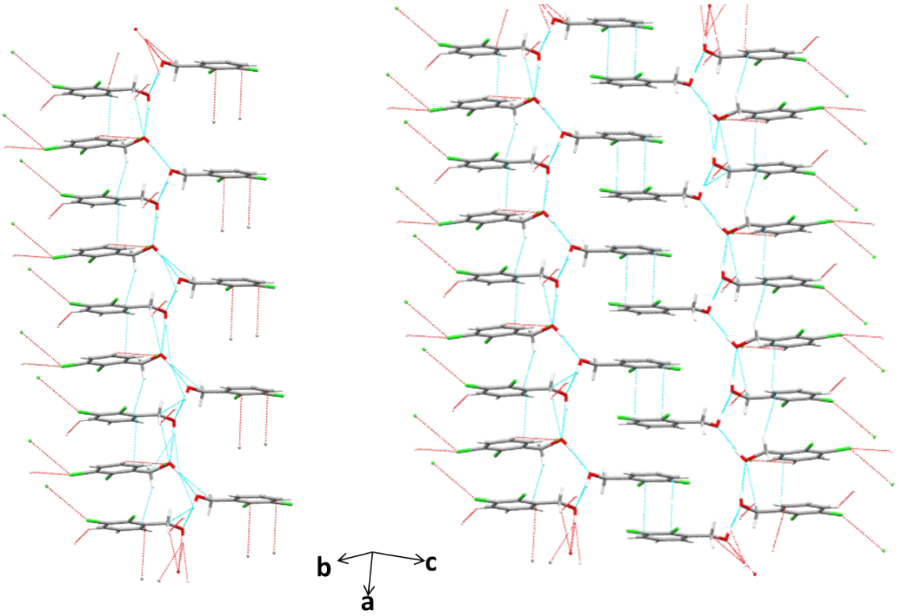


**Fig. S11** Packing diagram showing the linear and lateral assembly in the crystal of compound **7**.

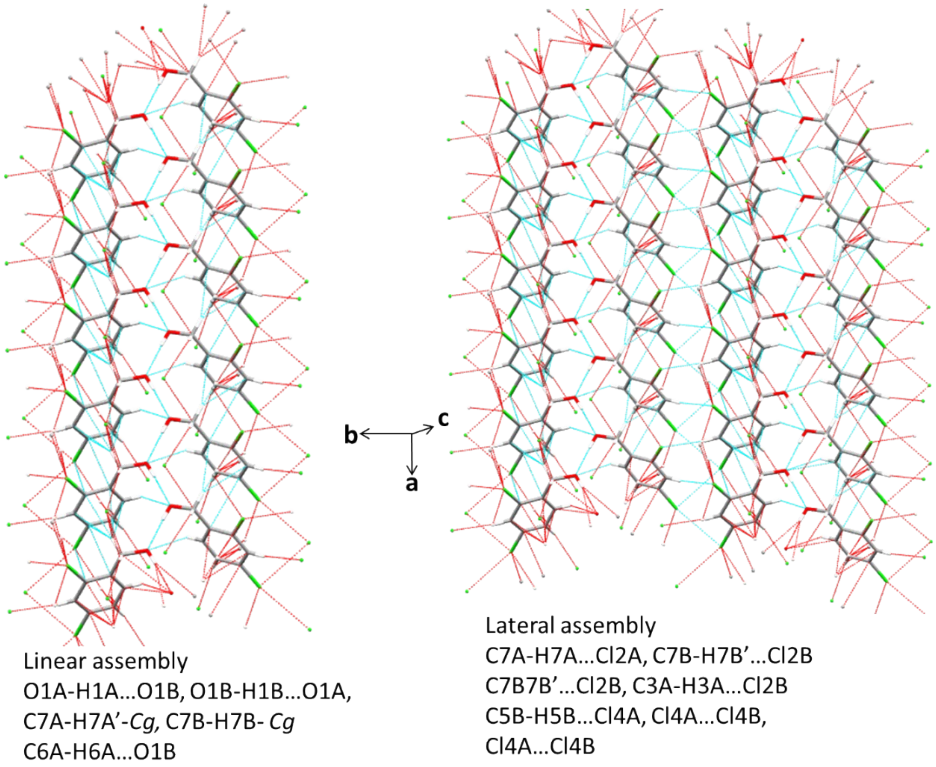


**Fig. S12** Packing diagram showing the linear and lateral assembly in the crystal of compound **8**.

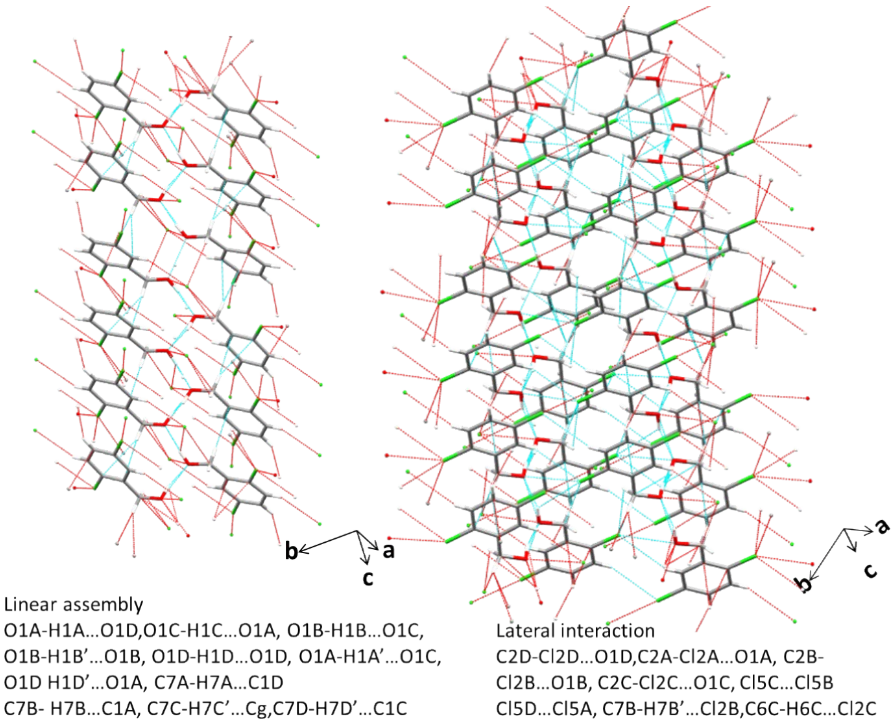


**Fig. S13** Packing diagram showing the linear and lateral assembly in the crystal of compound **9**.

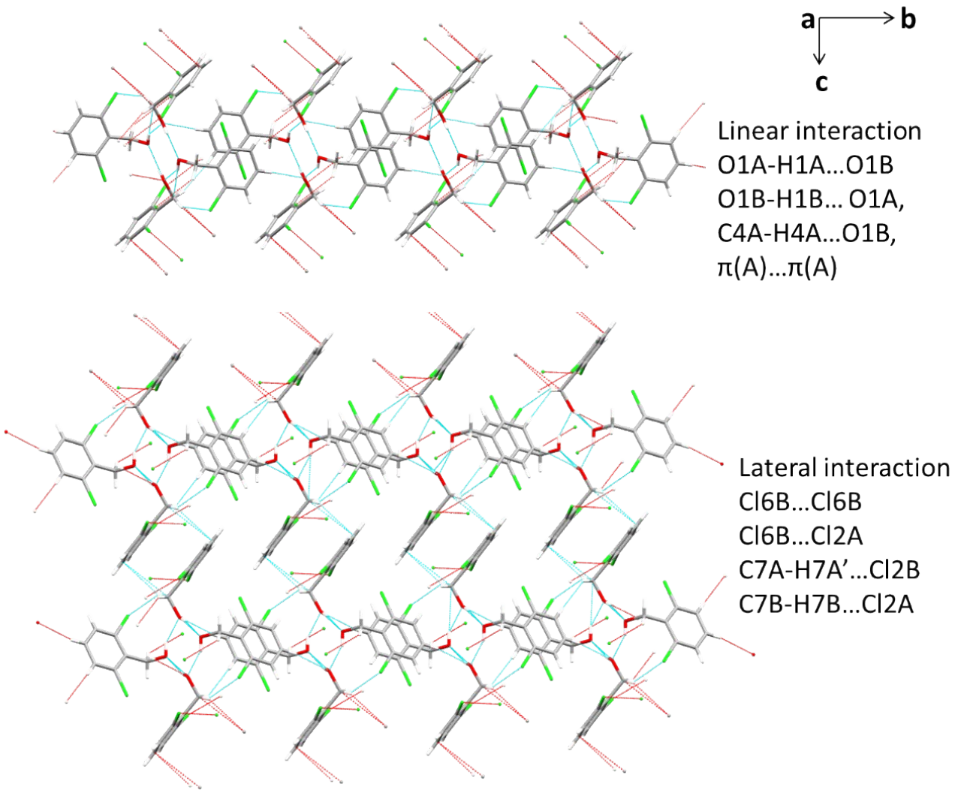


**Fig. S14** Packing diagram showing the linear and lateral assembly in the crystal of compound **10**.

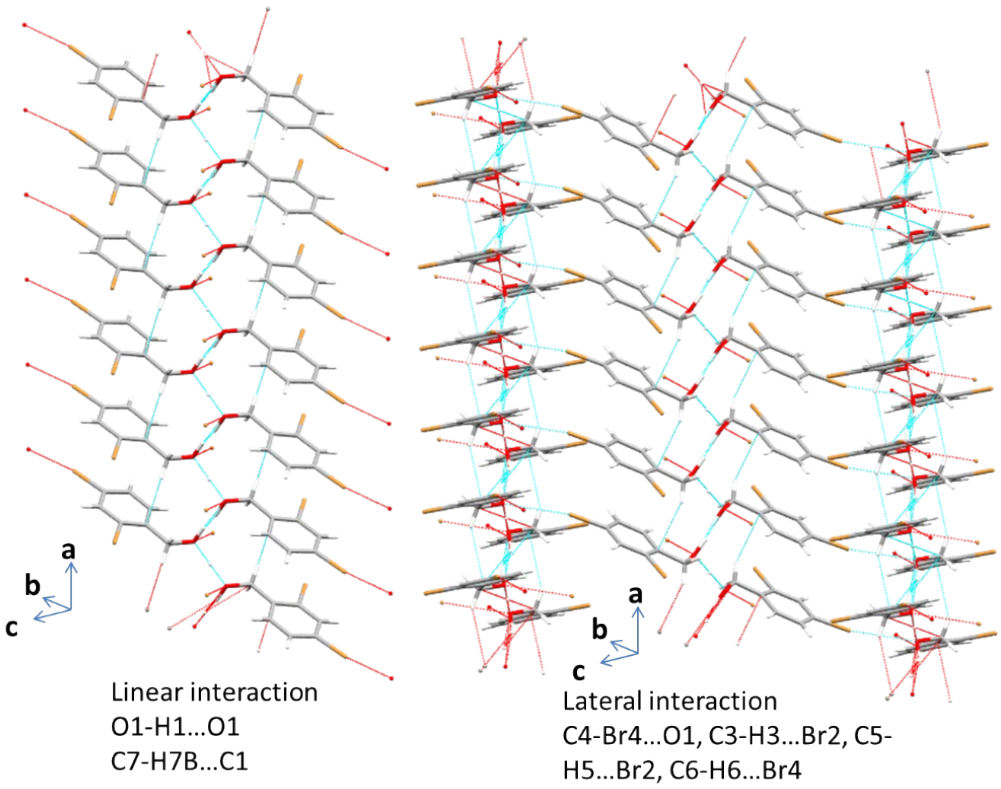


**Fig. S15** Packing diagram showing the linear and lateral assembly in the crystal of compound **11**. The disordered H-atoms are omitted for clarity.

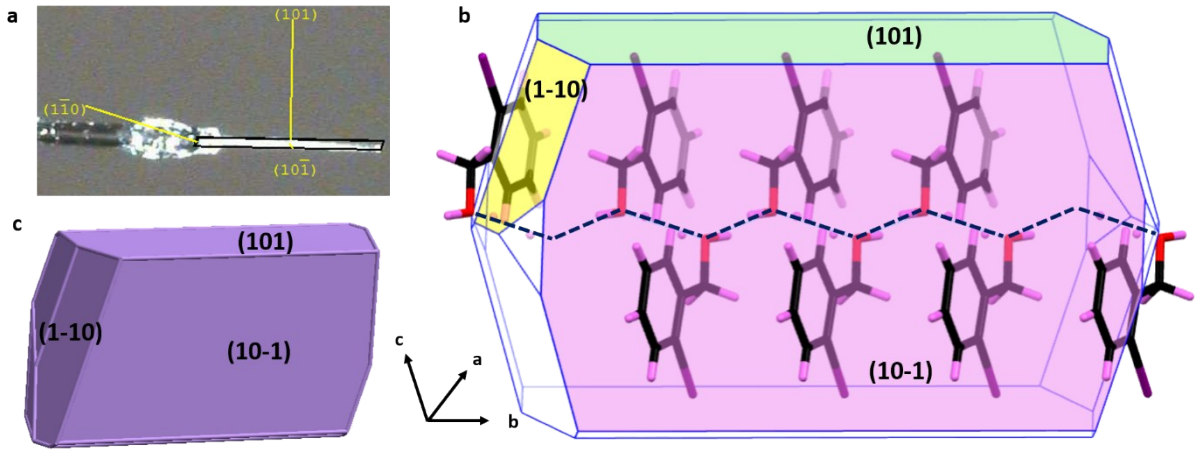


**Fig. S16** a) Face indexing of a single-crystal of compound **3** and the morphology calculated using b) BFDH method and c) ASE method for compound **3**. The crystal habits simulated from BFDH and ASE method are similar. The growth of crystal along the length [growing face is (1-10)] is facilitated by O-H…O hydrogen bonding (blue dotted lines). The disordered atoms are omitted for clarity.

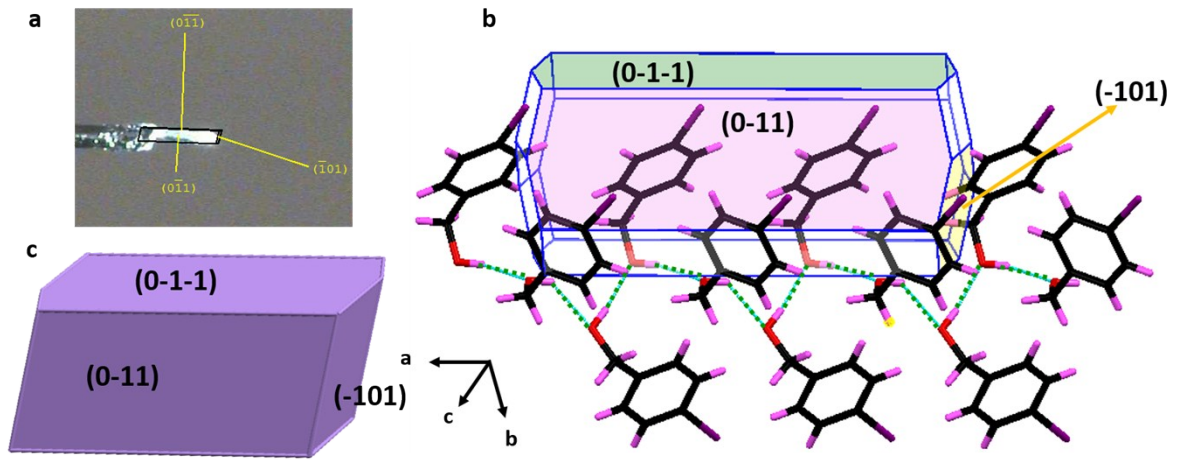


**Fig. S17** a) Face indexing of a single-crystal of compound **6** and the morphology calculated using b) BFDH method and c) ASE method for compound **6**. The crystal habits simulated from BFDH and ASE method are similar. The growth of crystal along the length [growing face is (-101)] is facilitated by O-H…O hydrogen bonding (green dotted lines). The disordered atoms are omitted for clarity.

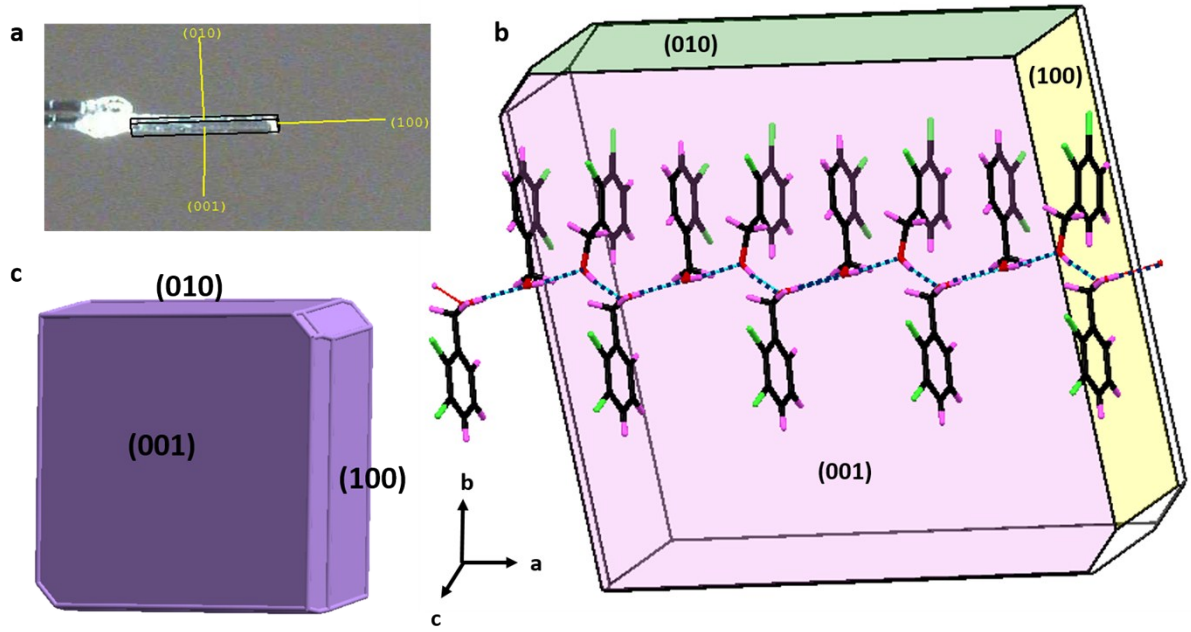


**Fig. S18** a) Face indexing of a single-crystal of compound **7** and the morphology calculated using b) BFDH method and c) ASE method for compound **7**. The crystal habits simulated from BFDH and ASE method are similar. The growth of crystal along the length [growing face is (100)] is facilitated by O-H…O hydrogen bonding (blue dotted lines).

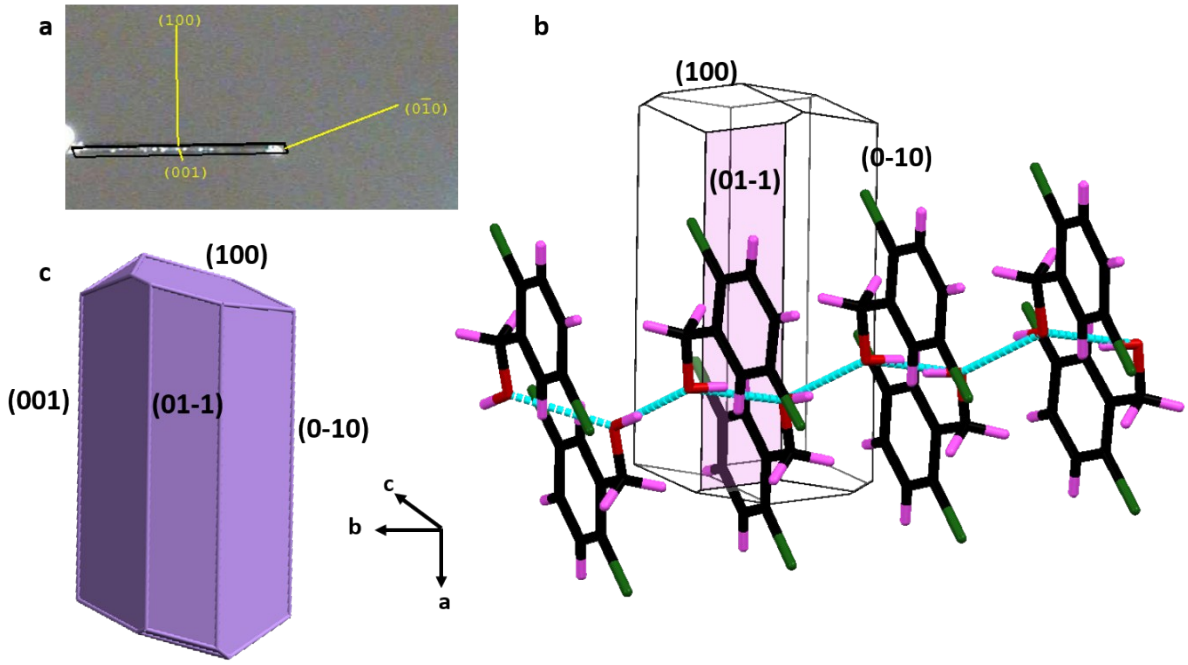


**Fig. S19** a) Face indexing of a single-crystal of compound **9** and the morphology calculated using b) BFDH method and c) ASE method for compound **9**. The crystal habits simulated from BFDH and ASE method are similar. The growth of crystal along the length [growing face is (0-10)] is facilitated by O-H…O hydrogen bonding. The disordered atoms are omitted for clarity.

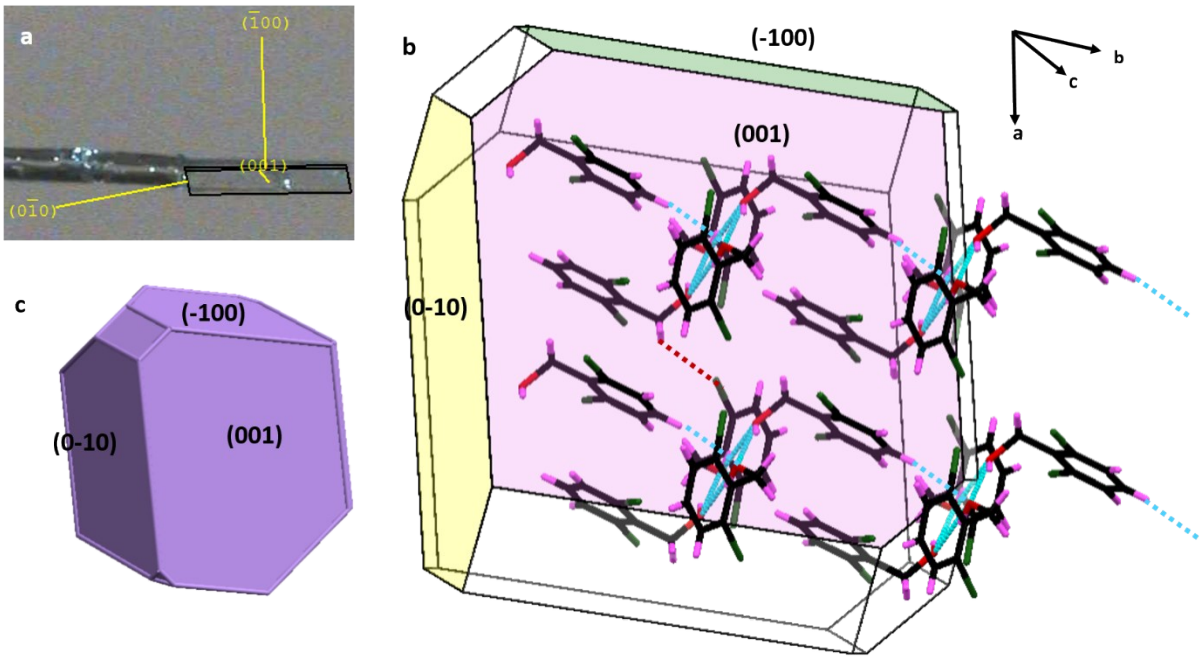


**Fig. S20** a) Face indexing of a single-crystal of compound **10** and the morphology calculated using b) BFDH method and c) ASE method for compound **10**. The crystal habits simulated from BFDH and ASE method are similar. The growth of crystal along the length [growing face is (0-10)] is facilitated by O-H…O and C-H…O hydrogen bonding (blue dotted lines).

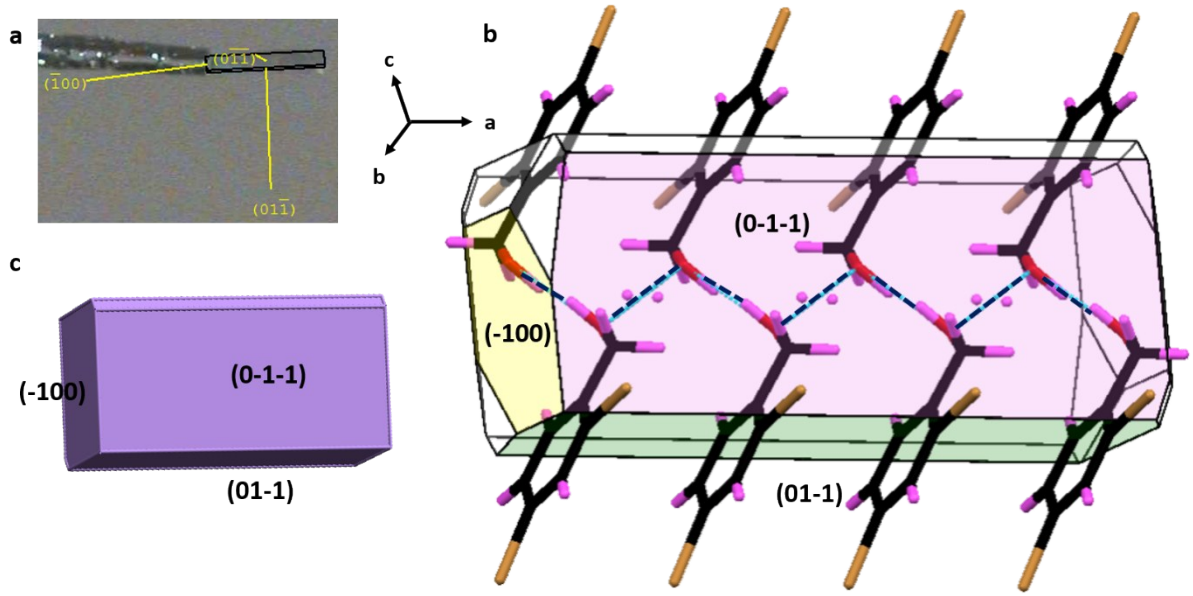


**Fig. S21** a) Face indexing of a single-crystal of compound **11** and the morphology calculated using b) BFDH method and c) ASE method for compound **11**. The crystal habits simulated from BFDH and ASE method are similar. The growth of crystal along the length [growing face is (-100)] is facilitated by O-H…O hydrogen bonding (blue dotted lines).

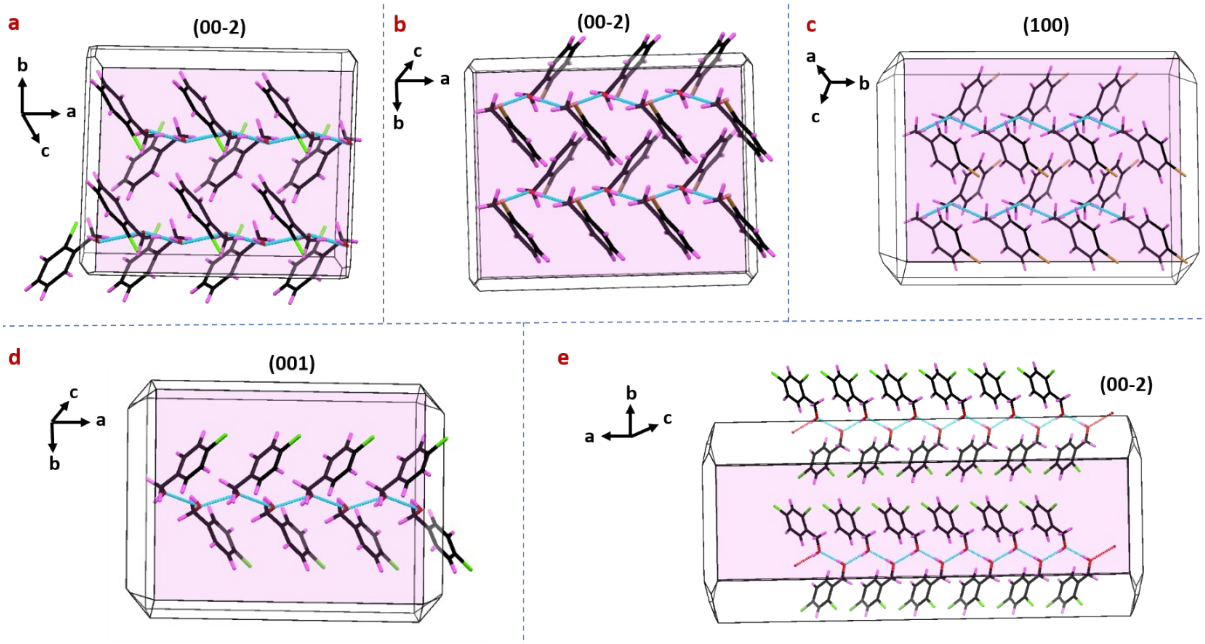


**Fig. S22** The crystal morphology calculated using BFDH method for compounds a) **1**, b) **2**, c) **4**, d) **5**, and e) **8**. The largest face (shown in pink and marked above each figure) is along the direction of hydrogen bonding in all the above cases. The CIF files for the above structures were downloaded from CCDC and the face indexing and ASEM studies were not carried out for the above cases.

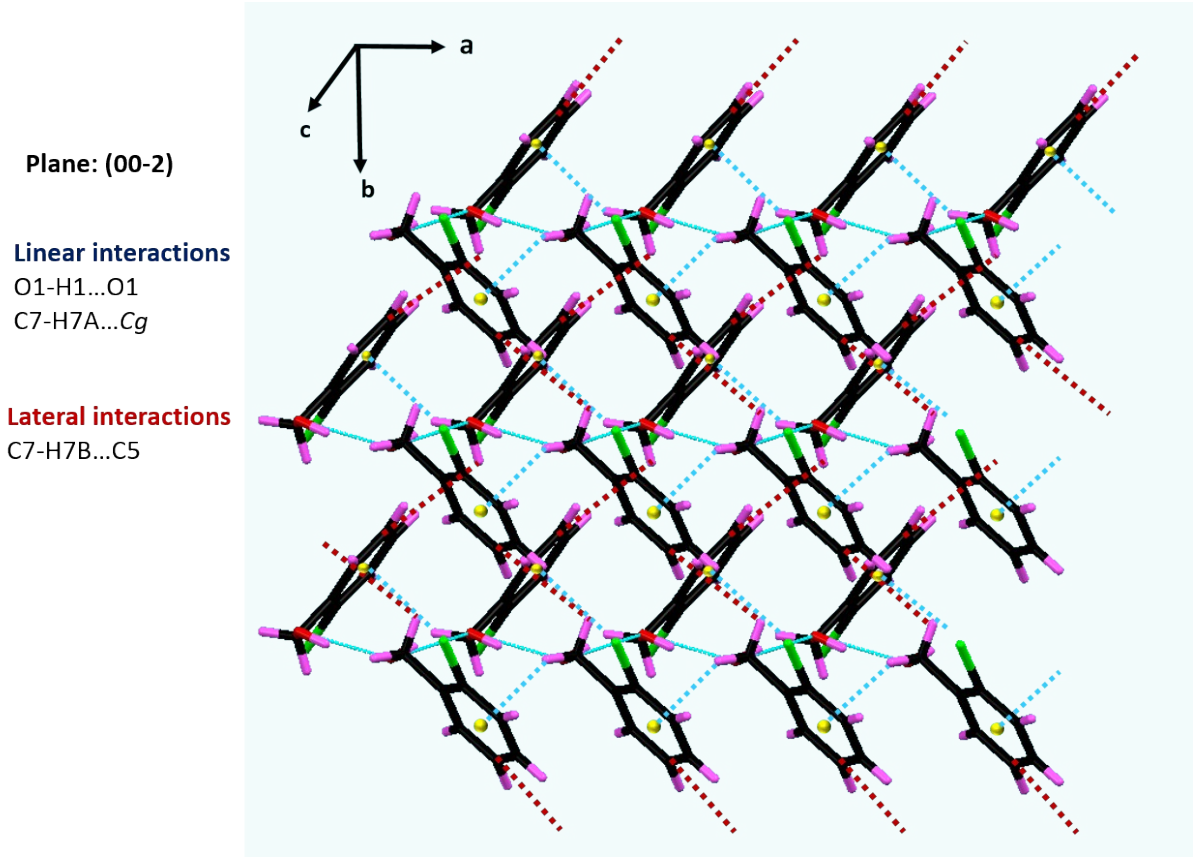


**Fig. S23** Packing diagram of compound **1** showing the linear and lateral interactions along the (00-2) plane.

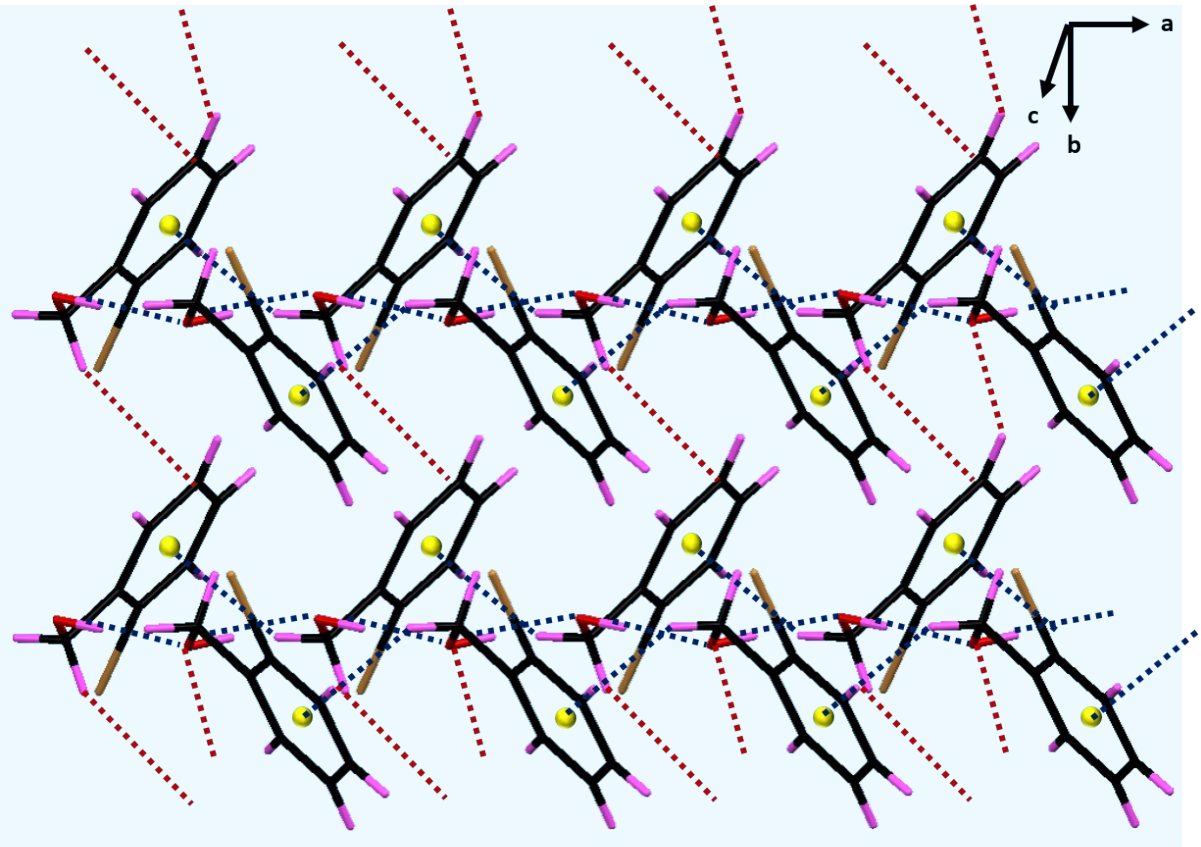


**Plane: (00-2)**

**Linear interactions**
O1-H1…O1
C7-H7A…*Cg*

**Lateral interactions**
C7-H7B…C5

**Fig. S24** Packing diagram of compound **2** showing the linear and lateral interactions along the (00-2) plane.

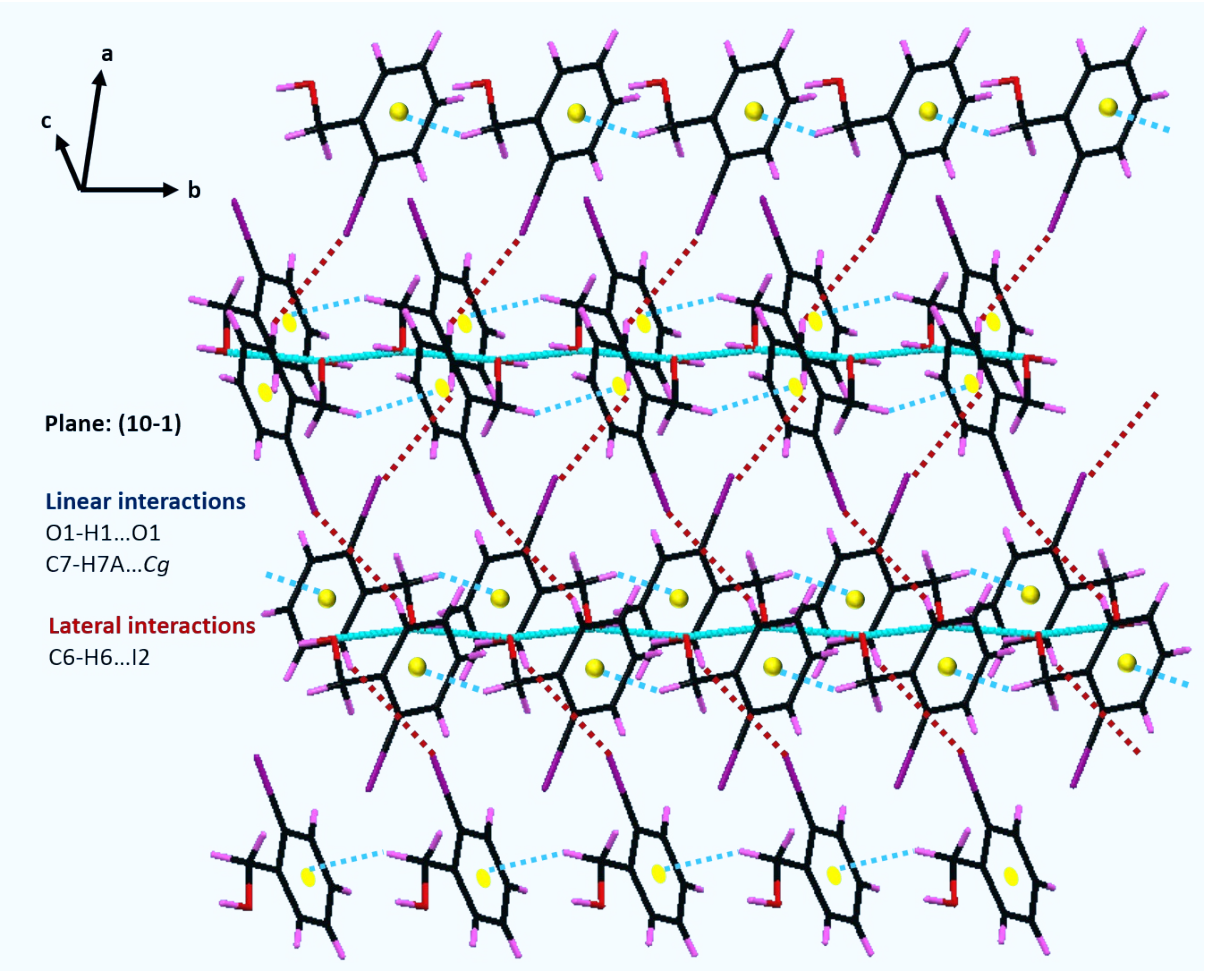


**Fig. S25** Packing diagram of compound **3** showing the linear and lateral interactions along the (10-1) plane.

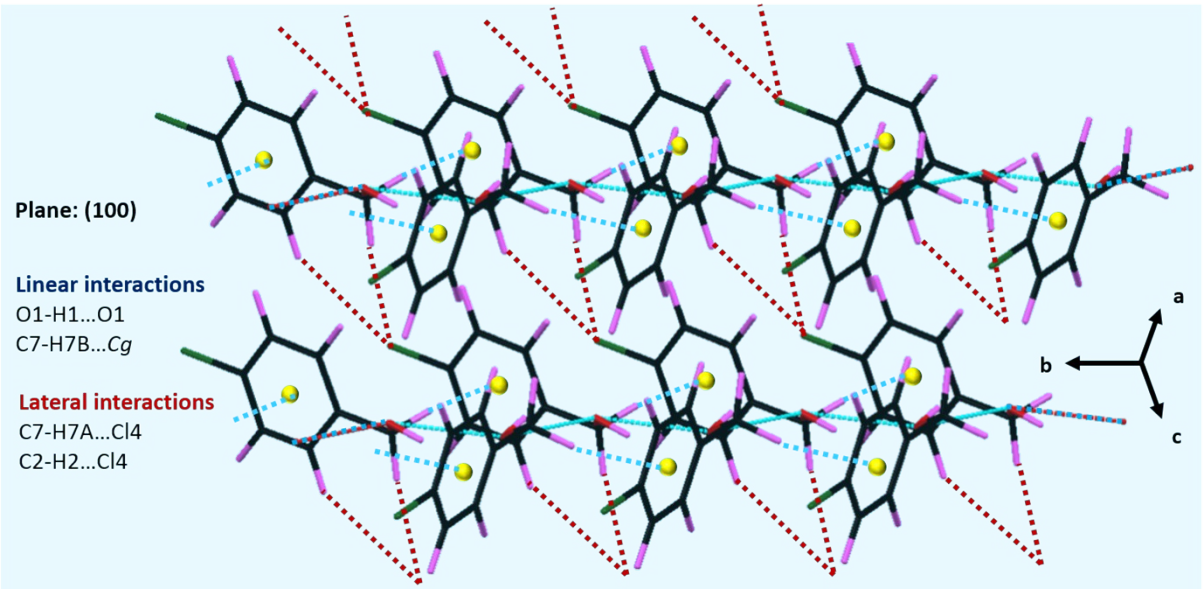


**Fig. S26** Packing diagram of compound **4** showing the linear and lateral interactions along the (100) plane.

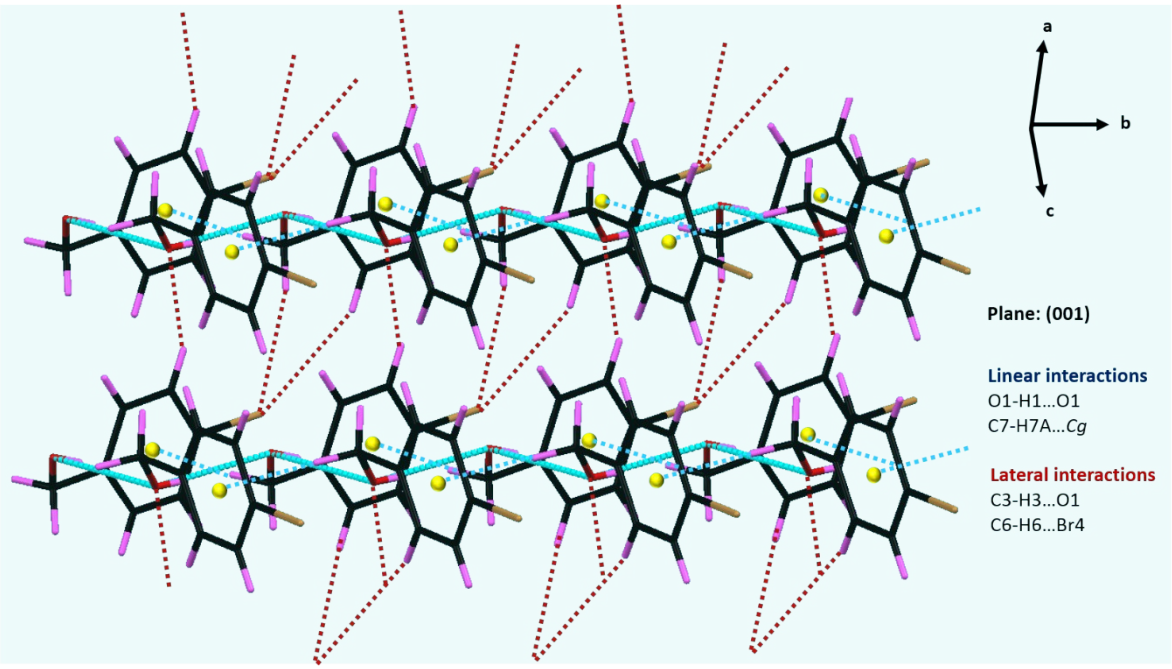


**Fig. S27** Packing diagram of compound **5** showing the linear and lateral interactions along the (001) plane.

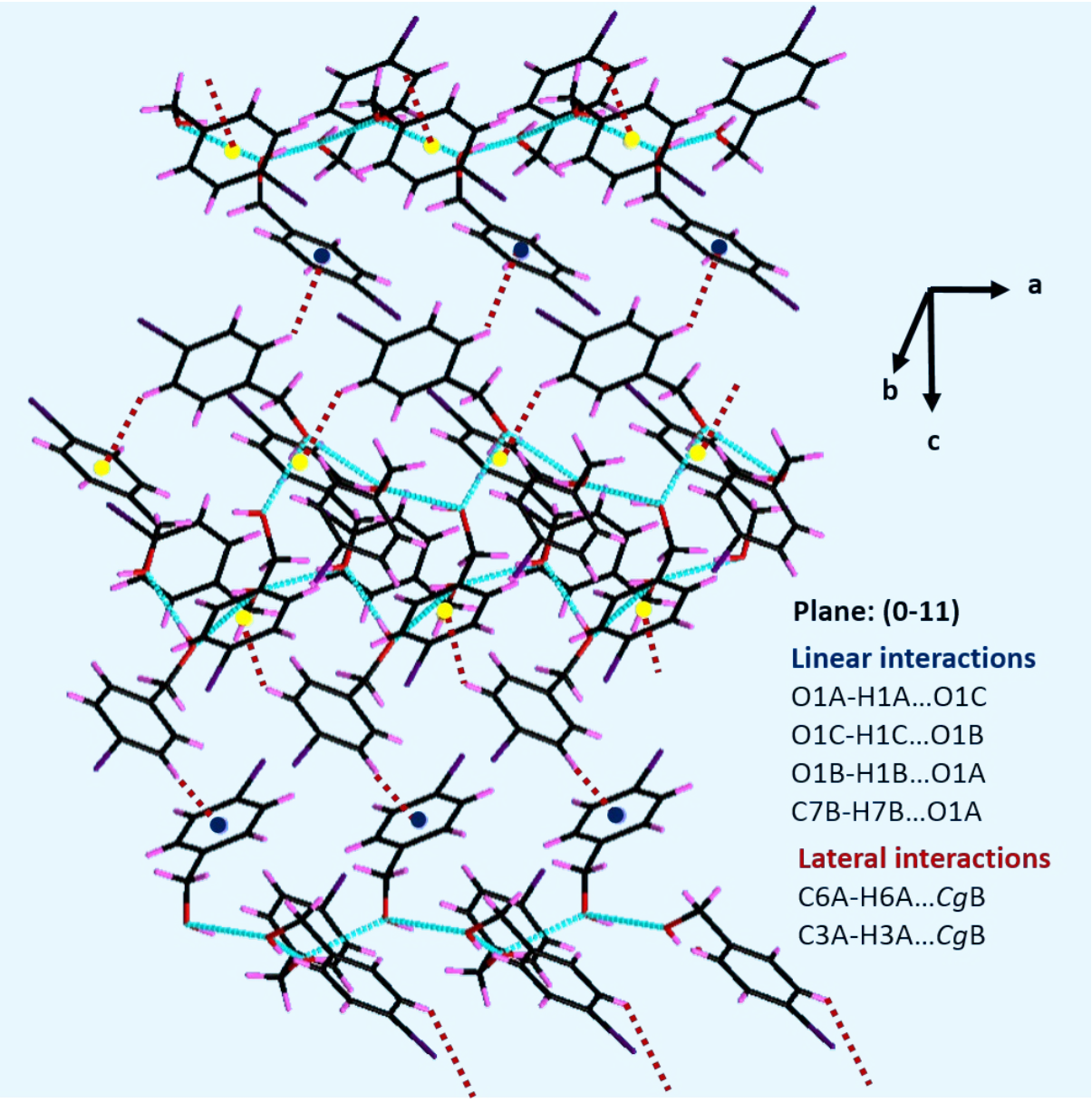


**Fig. S28** Packing diagram of compound **6** showing the linear and lateral interactions along the (0-11) plane.

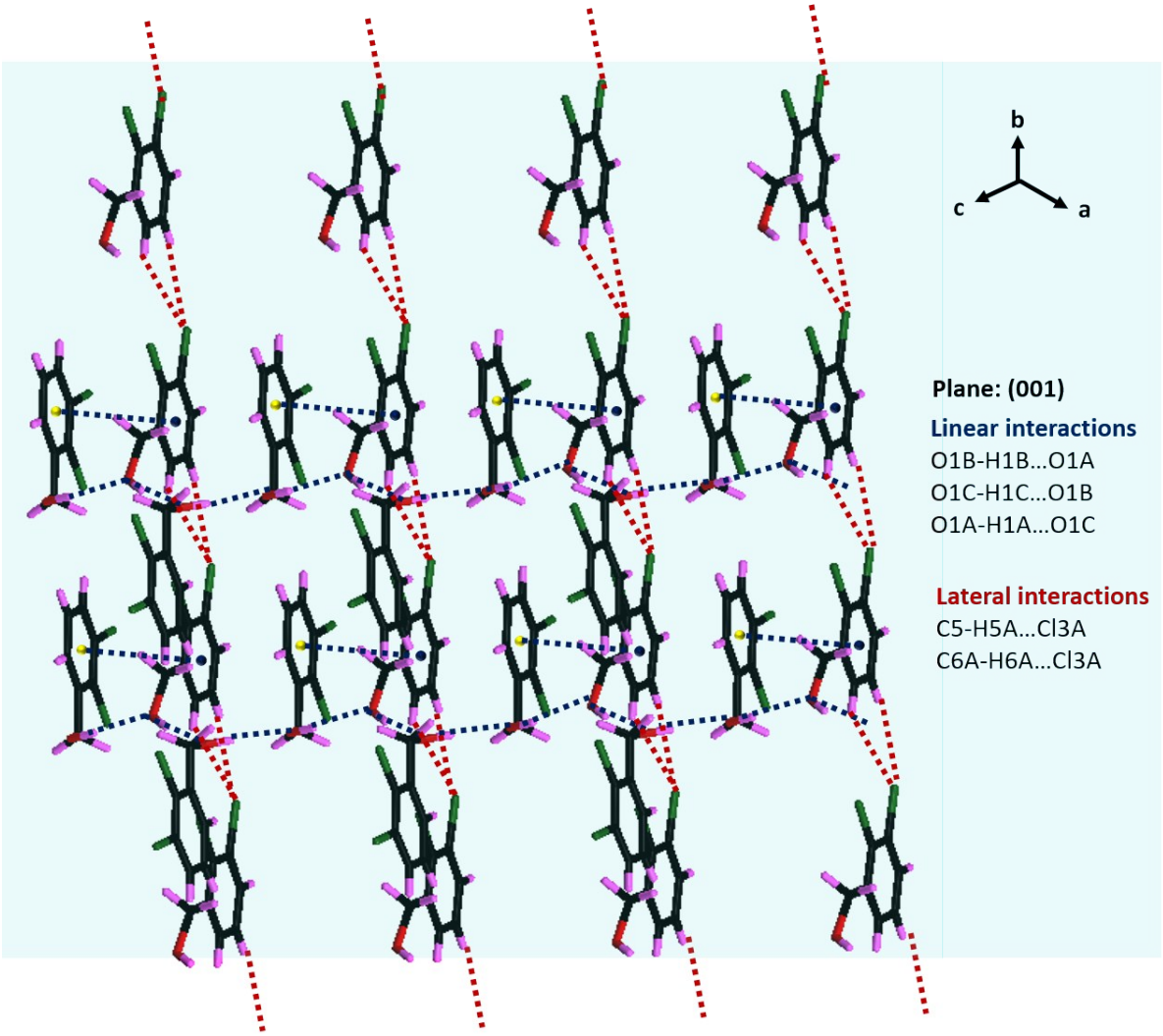


**Fig. S29** Packing diagram of compound **7** showing the linear and lateral interactions along the (001) plane.

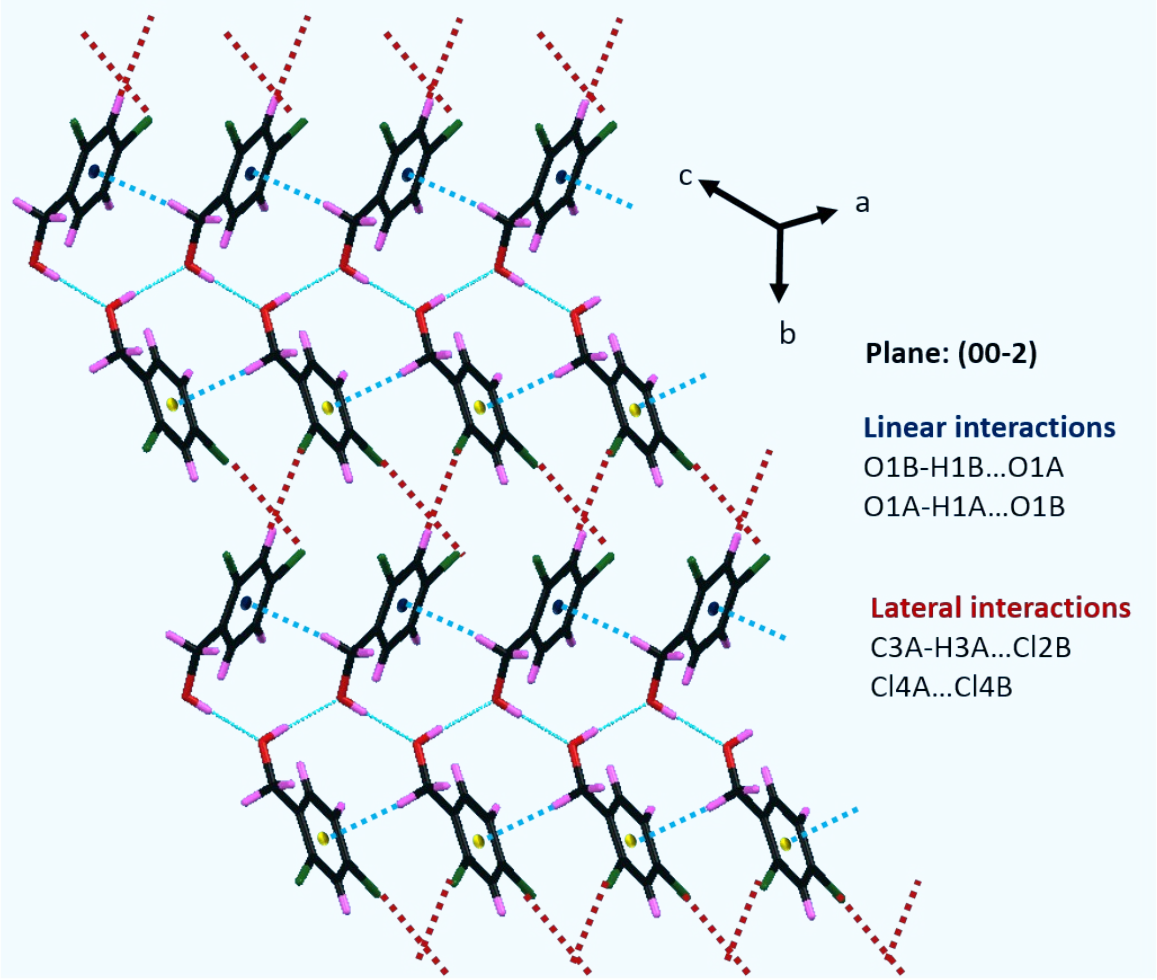


**Fig. S30** Packing diagram of compound **8** showing the linear and lateral interactions along the (00-2) plane.

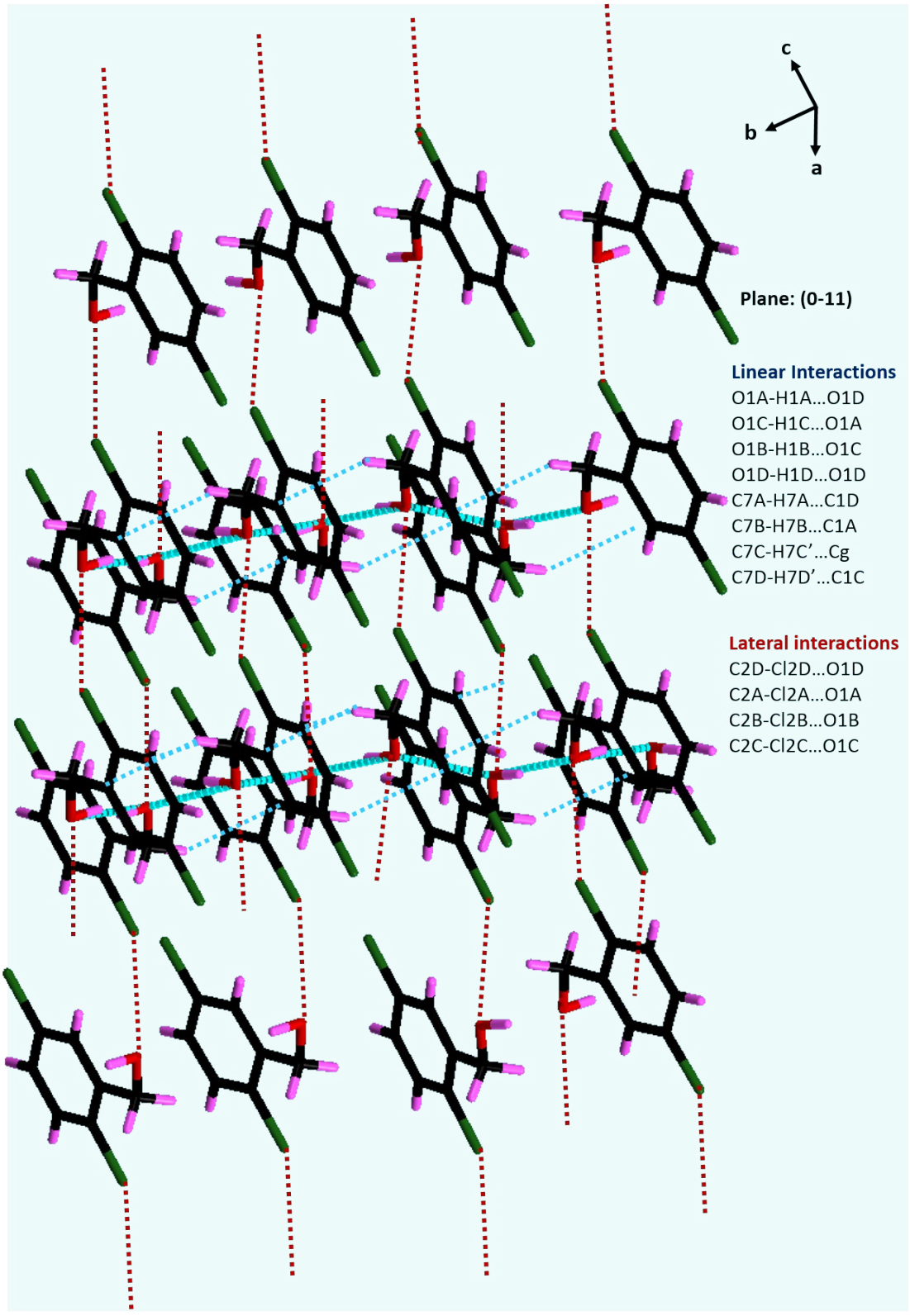


**Fig. S31** Packing diagram of compound **9** showing the linear and lateral interactions along the (0-11) plane.

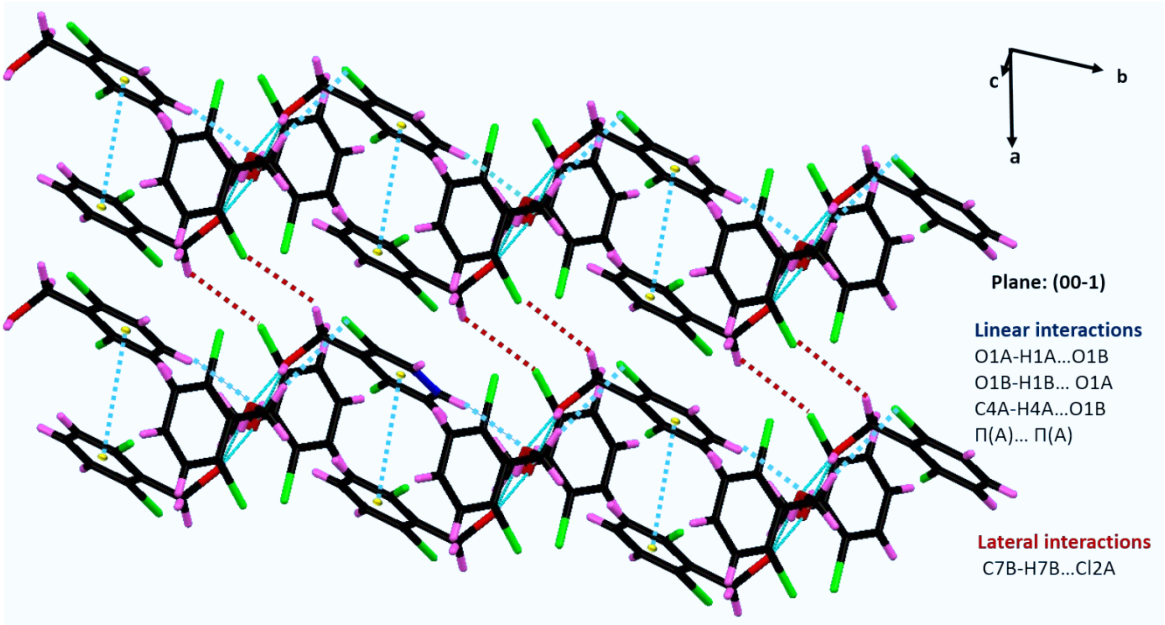


**Fig. S32** Packing diagram of compound **10** showing the linear and lateral interactions along the (00-1) plane.

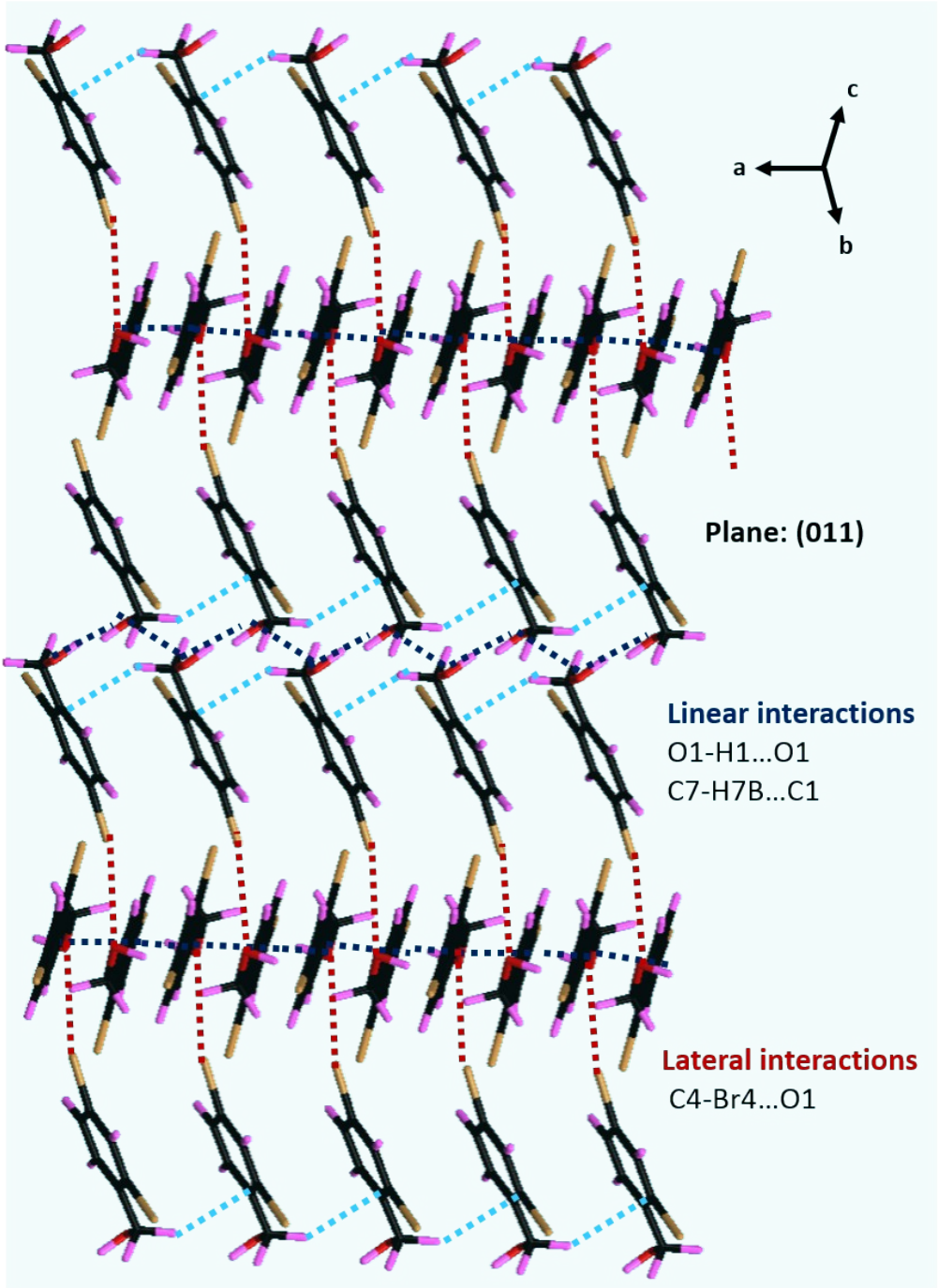


**Fig. S33** Packing diagram of compound **11** showing the linear and lateral interactions along the (011) plane.

**References:**


1. G. M. Sheldrick, *Acta Cryst.* 2008, **D64**, 112.
2. G. M. Sheldrick, (Date of access: 15/10/2014). SHELXL2014. University of Göttingen, Göttingen, Germany. URL http://shelx.uni-ac.gwdg.de/SHELX/ (2014).
3. P. McArdle, *J. Appl. Cryst*, 2017, **50**, 320; http://www.nuigalway.ie/crystallography/oscailsoftware/
4. D. R. Nunes, M. Reche-Tamayo, E. Ressouche, M. Raynal, B. Isare, P. Foury-Leylekian, P. –A. Albouy, P. Brocorens, R. Lazzaroni and L. Bouteiller, *Langmuir* 2019, **35**, 7970.
5. A. Vidyasagar, K. Handore and K. M. Sureshan, *Angew. Chem. Int. Ed.* 2011, **50**, 8021.